Inorganic Chemistry

Article

pubs.acs.org/IC

Construction of $(CuX)_{2n}$ Cluster-Containing (X = Br, I; n = 1, 2) Coordination Polymers Assembled by Dithioethers $ArS(CH_2)_mSAr$ (Ar = Ph, *p*-Tol; m = 3, 5): Effect of the Spacer Length, Aryl Group, and Metal-to-Ligand Ratio on the Dimensionality, Cluster Nuclearity, and the Luminescence Properties of the Metal−Organic Frameworks

Michael Knorr,*[,†] Fabrice Guyon,[†] Abderrahim Khatyr,[†] Carsten Strohmann,[‡] Magali Allain,[§] Shawkat M. Aly,[⊥,∥] Antony Lapprand,[∥] Daniel Fortin,[∥] and Pierre D. Harvey*[,∥]

[†]Institut UTINAM, UMR CNRS 6213, Faculté des Sciences et des Techniques, Université de Franche-Comté, 16 Route de Gray, 25030 Besançon, France

[‡]Anorganische Chemie, Technische Universität Dortmund, Otto-Hahn-Strasse 6, D-44227 Dortmund, Germany

[§]Laboratoire MOLTECH-Anjou UMR CNRS 6200, Université d'Angers, 2 Boulevard Lavoisier, 49045 Angers, France

[∥]Departement de Chimie, Université de Sherbrooke, 2550 Boulevard Université, Sherbrooke, Quebec, Canada J1K 2R1

Supporting Information

ABSTRACT: Reaction of CuI with bis(phenylthio)propane in a 1:1 ratio yields the two-dimensional coordination polymer $[\{Cu(\mu_2\text{-}I)_2Cu\}\{\mu\text{-}PhS(CH_2)_3SPh\}_2]_n$ (**1**). The 2D-sheet structure of **1** is built up by dimeric Cu_2I_2 units, which are connected via four bridging 1,3-bis(phenylthio)propane ligands. In contrast, treatment of 2 equiv of CuI with 1,3-bis(phenylthio)propane in MeCN solution affords in a self-assembly reaction the strongly luminescent metal−organic 2D-coordination polymer $[Cu_4I_4\{\mu\text{-}PhS(CH_2)_3Ph\}_2]_n$ (**2**), in which cubane-like $Cu_4(\mu_3\text{-}I)_4$ cluster units are linked by the dithioether ligands. The crystallographically characterized one-dimensional (1D) compound $[\{Cu(\mu_2\text{-}Br)_2Cu\}\{\mu\text{-}PhS(CH_2)_3SPh\}_2]_n$ (**3**) is obtained using CuBr. The outcome of the reaction of $PhS(CH_2)_5SPh$ with CuI also depends of the metal-to-ligand ratio employed. Mixing CuI and the dithioether in a 2:1 ratio results in formation of $[Cu_4I_4\{\mu\text{-}PhS(CH_2)_5Ph\}_2]_n$ (**4**) in which cubane-like $Cu_4(\mu_3\text{-}I)_4$ clusters are linked by the bridging dithioether ligand giving rise to a 1D necklace structure. A ribbon-like 1D-polymer with composition $[\{Cu(\mu_2\text{-}I)_2Cu\}\{\mu\text{-}PhS(CH_2)_5SPh\}_2]_n$ (**5**), incorporating rhomboid Cu_2I_2 units, is produced upon treatment of CuI with 1,5-bis(phenylthio)pentane in a 1:1 ratio. Reaction of CuBr with $PhS(CH_2)_5SPh$ produces the isomorphous 1D-compound $[\{Cu(\mu_2\text{-}Br)_2Cu\}\{\mu\text{-}PhS(CH_2)_5SPh\}_2]_n$ (**6**). Strongly luminescent $[Cu_4I_4\{\mu\text{-}p\text{-}TolS(CH_2)_5STol\text{-}p\}_2]_n$ (**7**) is obtained after mixing 1,5-bis(*p*-tolylthio)pentane with CuI in a 1:2 ratio, and the 2D-polymer $[\{Cu(\mu_2\text{-}I)_2Cu\}_2\{\mu\text{-}p\text{-}TolS(CH_2)_5STol\text{-}p\}_2]_n$ (**8**) results from reaction in a 1:1 metal-to-ligand ratio. Under the same reaction conditions, 1D-polymeric $[\{Cu(\mu_2\text{-}Br)_2Cu\}\{\mu\text{-}p\text{-}TolS(CH_2)_5STol\text{-}p\}_2]_n$ (**9**) is formed using CuBr. This study reveals that the structure of the self-assembly process between CuX and $ArS(CH_2)_mSAr$ ligands is hard to predict. The solid-state luminescence spectra at 298 and 77 K of **2** and **4** exhibit very strong emissions around 535 and 560 nm, respectively, whereas those for **1** and **5** display weaker ones at about 450 nm. The emission lifetimes are longer for the longer wavelength emissions (>1.0 μs arising from the cubane species) and shorter for the shorter wavelength ones (<1.4 μs arising from the rhomboid units). The Br-containing species are found to be weakly fluorescent.

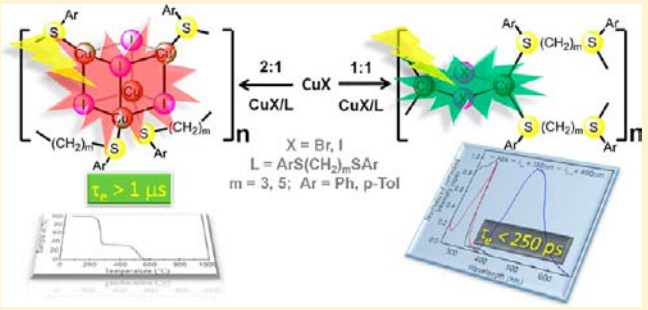

INTRODUCTION

The coordination mode of aromatic dithioether ligands of the type $PhS(CH_2)_nSPh$, which may be considered as the sulfur analogues of the ubiquitous diphosphanes $Ph_2P(CH_2)_nPPh_2$, depends in a sensible manner from the number of methylene units in the $(CH_2)_n$ chain. In the case of $PhS(CH_2)_nSPh$ where n = 1, a η^1-bonding mode with Rh, Pd, and Pt is sometimes encountered. Such examples for this monodendate coordination mode are $[(\eta^5\text{-}C_5Me_5)IrCl_2(\eta^1\text{-}PhSCH_2SPh)\}]$, *trans*-$[PdCl_2(\eta^1\text{-}PhSCH_2SPh)_2]$, and *cis*-$[PtCl_2(\eta^1\text{-}PhSCH_2SPh)_2]$.[1] In addition, bis(phenylthio)-methane is known to act as bridging ligand, thus assembling polynuclear compounds.[2]

Although 1,2-bis(phenylthio)ethane and 1,3-bis(phenylthio)-propane may also adopt a bridging coordination mode in some coordination polymers, the formation of stable five- or six-membered

Received: June 30, 2012
Published: September 6, 2012

   dx.doi.org/10.1021/ic301385u | *Inorg. Chem.* 2012, 51, 9917−9934

chelate complexes is in general preferred for $n = 2$ or 3. Some representative examples for this chelating coordination mode are *cis*-$[PtCl_2\{PhS(CH_2)_nSPh\}_2]$ (n = 2, 3), tetrahedral $[Cu\{PhS(CH_2)_nSPh\}_2][BF_4]$ (n = 2, 3), and octahedral compounds $[SnCl_4\{PhS(CH_2)_3SPh\}_2]$ and $[Ru(phen)_2\{PhS(CH_2)_nSPh\}]$.[3] A series of polymorphous supramolecular complexes of type $[Au_2Cl_2\{PhS(CH_2)_3SPh\}]$ is formed by reaction of 1,3-bis(phenylthio)propane with $HAuCl_4 \cdot 3H_2O$.[4] However, a significant change is noticed when the number of methylene units reaches n = 4, 5, and 6. A relationship between the ligand chain length and the structure using a $PdCl_2$ fragment has been established by Sanger et al. On the basis of IR data, the formation of ligand-bridged palladium complexes of trans-geometry has been proposed for $n = 4-6$.[5] Recently, an X-ray diffraction study on $[Pd\{PhS(CH_2)_5SPh\}Cl_2]_n$ confirmed that 1,5-bis(phenylthio)pentane spans indeed the Pd-centers giving rise to a polymeric chain complex.[6] The crystal engineering with this flexible ligand on Ag(I) salts under different conditions (varying the solvent, metal-to-ligand ratios, and counterions) gave rise to a number of two-dimensional (2D) frameworks with fascinating structural motifs.[7] The structural diversity and modulation of coordination architectures with flexible dithioether ligands has been recently reviewed by Bu and Li.[8]

It is well established that interaction of various nucleophiles (L) such as aniline and pyridyl type ligands and phosphanes with copper(I) halides often affords in a self-assembly process tetranuclear cubane-like $Cu_4X_4L_4$ cluster exhibiting remarkable photophysical properties.[9,10] Alternatively, dinuclear compounds possessing a rhomboid Cu_2X_2 core may be formed.[11] Interestingly, complexes containing the $Cu_2I_2N_4$ core exhibit a large flexibility of the Cu···Cu separations similar to that found for $Cu_2I_2S_4$-containing compounds. These may vary between 3.364(5) Å in $[\{CuI(quinolone)_2\}_2]$[11a] to 2.647 Å in the polymeric $[Cu_2I_2(dps)_2]_n$ (dps = *N*-bound dipyridylsulfide).[11c] In the context of bi- and polydentate thioether ligands, we recently reported the reactivity of the aromatic dithioether ligands $PhS(CH_2)_mSPh$ (m = 1, 2, 4) toward CuI to evaluate the influence of the spacer on the resulting framework. For bis(phenylthio)methane, a strongly luminescent coordination polymer $[Cu_4I_4\{\mu\text{-}PhS_2CH_2SPh\}_2]_n$, in which $Cu_4(\mu_3\text{-}I)_4$ cluster units are linked by the dithioether ligand in a one-dimensional (1D) necklace structure, was isolated. Concurrently, the reaction of $PhSCH_2CH_2SPh$ with CuI resulted in formation of the metallopolymer $[(CuI)_2\{\mu\text{-}PhS(CH_2)_2SPh\}_2]_n$, whose 2D-network is built up upon dimeric Cu_2I_2 units, which are interconnected via bridging dithioether ligands.[12a] Using the more flexible 1,4-$PhS(CH_2)_4SPh$ dithioether ligand afforded the strongly luminescent metal−organic 2D coordination polymer $[Cu_4I_4\{\mu\text{-}PhS(CH_2)_4SPh\}_2]_n$ whose interpenetrated 2D network is built upon by $Cu_4(\mu_3\text{-}I)_4$ cubane-like clusters as secondary building units (SBUs), interconnected via bridging bis(phenylthio)butane ligands.[12b,13]

To examine the effect of an insertion of additional spacer units between the SAr groups on the dimensionality, cluster nuclearity, and the luminescence properties of the metal−organic framework (MOF), the 1,3-bis(phenylthio)propane and the more flexible 1,5-bis(phenylthio)pentane ligands were also studied. The impact of the substitution pattern of the aryl cycle on the resulting polymer structure is also investigated. In contrast with the growing number of reports dealing with the coordination of acyclic dithioethers on CuI,[13−15] reports on the ligation on CuBr are extremely scarce.[16] We now wish to report a comparison study on the coordination chemistry of $ArS(CH_2)_mSAr$ toward copper(I) bromide vs copper(I) iodide. The crystal structures of new polymeric materials using the flexible $ArS(CH_2)_mSAr$ ligands and CuX (Ar = Ph, *p*-Tol; m = 3, 5; X = Br, I) are reported along with a thermal stability study and their photophysical properties. 1D vs 2D polymers, Cu_2I_2 vs Cu_4I_4 clusters are obtained in a predictable fashion, and the -$(CH_2)_5$- materials are more thermally stable than those with -$(CH_2)_3$-. Furthermore, the Cu_2I_2-containing polymers exhibit a structured emission band at 450 nm with emission lifetimes <1.4 μs, whereas the Cu_4I_4-containing ones emit in the 500−600 nm window as a featureless band with emission lifetimes >1.0 μs. Finally, the Cu_2Br_2-containing polymers emit only weakly, and the presence of fluorescence has been demonstrated. The list of the investigated coordination polymers is shown in Chart 1.

Chart 1. Investigated Coordination Polymers

Polymer	Cluster	Ligand	CuX:ligand ratio	Dimensionality
1	Cu_2I_2	$PhS(CH_2)_3SPh$	1:1	2D
2	Cu_4I_4	$PhS(CH_2)_3SPh$	2:1	2D
3	Cu_2Br_2	$PhS(CH_2)_3SPh$	1:1	1D
4	Cu_4I_4	$PhS(CH_2)_5SPh$	2:1	1D
5	Cu_2I_2	$PhS(CH_2)_5SPh$	1:1	1D
6	Cu_2Br_2	$PhS(CH_2)_5SPh$	1:1	1D
7	Cu_4I_4	$pTolS(CH_2)_5SpTol$	2:1	?
8	Cu_2I_2	$pTolS(CH_2)_5SpTol$	1:1	2D
9	Cu_2Br_2	$pTolS(CH_2)_5SpTol$	1:1	1D

RESULTS AND DISCUSSION

Reaction of CuI with 1,3-Bis(phenylthio)propane. Upon treatment of a solution of 1,3-bis(phenylthio)propane in MeCN with an equimolar amount of CuI at room temperature, colorless crystals are formed within 2 days. Elemental analysis of this air-stable material is consistent with the coordination of 1 dithioether ligand per CuI unit. Indeed, an X-ray diffraction study reveals the presence of a 2D coordination polymer $[\{Cu(\mu_2\text{-}I)_2Cu\}_2\{\mu\text{-}PhS(CH_2)_3SPh\}_2]_n$ (**1**) (Scheme 1 and Figure 1, a view of the dinuclear $Cu(\mu_2\text{-}I)_2Cu$ motif of **1** is given in the Supporting Information). The framework consists of centrosymmetric $Cu_2(\mu_2\text{-}I)_2$ rhomboid dimers connected to an adjacent unit via one μ_2-bridging dithioether ligand. Each Cu atom exhibits a distorted tetrahedral environment, coordinated by two bridging iodide ligands and two thioether groups of two distinct ligands. The 2D-network resulting from this coordination mode includes centrosymmetric 28-membered macrocycles constituted by four dithioether ligands, six Cu atoms, and two iodide ligands.

Overall, the coordination mode is reminiscent to that encountered in coordination polymer $[\{Cu(\mu_2\text{-}I)_2Cu\}_2\{\mu\text{-}PhS(CH_2)_2SPh\}_2]_n$.[12a] The Cu···Cu separation of **1** is similar to that observed in $[\{Cu(\mu_2\text{-}I)_2Cu\{\mu\text{-}PhS(CH_2)_2SPh\}_2]_n$ [2.826(10) vs 2.8058(11) Å]. Other complexes exhibiting a rhomboidal Cu_2I_2 unit and weak Cu···Cu interactions close to the values of $[\{Cu(\mu_2\text{-}I)_2Cu\}\{\mu\text{-}PhS(CH_2)_mSPh\}_2]_n$ (m = 2, 3) have been reported for $[Cu_2I_2[16]aneS_4]_n$ ([16]aneS$_4$ = 1,5,9,13-tetrathiacyclohexadecane) (2.8079(12) Å and dinuclear $[\{MeSi(CH_2SMe)_3\}CuI]_2$ (2.862(2) Å).[17,18] A literature survey reveals that similarly to the $Cu_2I_2N_4$ complexes, the Cu···Cu separation in the $Cu_2I_2S_4$ species is quite variable.[11f] An example in the short-range below the sum of van der Waals radii of two Cu atoms (2.8 Å) is given by a dithioether-functionalized tetrathiafulvalene complex and $[(tht)_2Cu(\mu\text{-}I)_2Cu(tht)_2]$ (tht = tetrahydrothiophene) with separations of only 2.6469(15) and 2.675 Å, respectively.[19,20]

dx.doi.org/10.1021/ic301385u | *Inorg. Chem.* 2012, 51, 9917−9934

Scheme 1

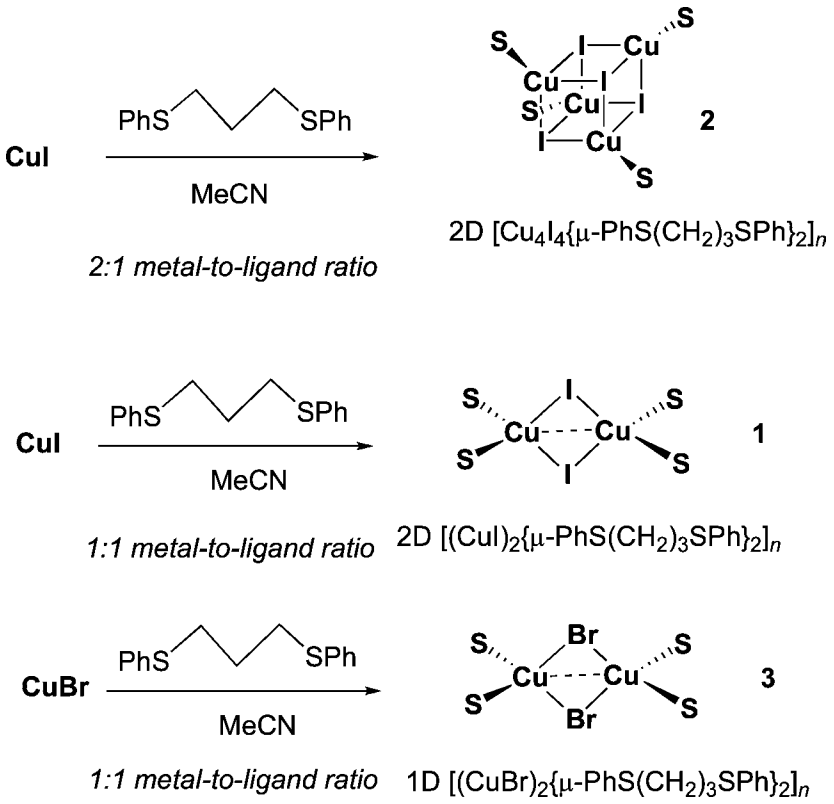

Changing of the molar CuI-to-ligand ratio to 2:1 using the same experimental conditions has a dramatic effect on the composition of the colorless crystalline material, which is isolated in 52% yield from cold MeCN. The elemental analyses are now consistent with the ligation of two CuI units per dithioether. The comparison of the emission spectra of this strongly luminescent material (see below) with those for the polymers $[Cu_4I_4\{\mu\text{-}PhSCH_2SPh\}_2]_n$,[12a] $[Cu_4I_4\{\mu\text{-}PhS(CH_2)_4SPh\}_2]_n$,[12b] and $[Cu_4I_4\{\mu\text{-}PhS(CH_2)_5SPh\}_2]_n$ (**4**) (see below), in which the occurrence of $Cu_4(\mu_3\text{-}I)_4$ clusters as SBUs has been crystallographically established, lets also suggest the existence of cubane-like $Cu_4(\mu_3\text{-}I)_4$ cores in compound **2** (Scheme 1).

Noteworthy, in the case of $[Cu_4I_4\{\mu\text{-}PhS(CH_2)_mSPh\}_2]_n$ (m = 1, 4), the variation of the CuI-to-ligand ratio had no influence on the composition of the resulting material.[12] Crystals of suitable quality for X-ray analysis were obtained, which confirmed indeed the presence of tetranuclear $Cu_4(\mu_3\text{-}I)_4$ SBUs. As shown in Figure 2, the self-assembly process affords a 2D network, where in each layer a $PhS(CH_2)_2SPh$ ligand spans two adjacent $Cu_4(\mu_3\text{-}I)_4$ clusters, generating 28-membered square grids. The mean Cu−S bond length of 2.3112 Å lies in a similar range as that of $[Cu_4I_4\{\mu\text{-}PhS(CH_2)_5SPh\}_2]_n$ (**4**) (2.299 Å), but is shorter than that of $[\{Cu(\mu_2\text{-}I)_2Cu\}_2\{\mu\text{-}PhS(CH_2)_3SPh\}_2]_n$ (**1**) (2.3465 Å). Within the slightly distorted closed cubane-type cluster, the mean distance of 2.7272(12) Å (at 293 K) between the 4 nonequivalent Cu centers is clearly below the sum of the van der Waals radii between two Cu atoms and indicates a bonding interaction (Figure 4**A**). Using the CrystalMaker Software (version 8.6.2), the porosity (corrected for first-nearest-neighbor sphere overlap and site visibility) of **1** has been calculated: filled space: 642.063 Å^3 (16.68%) per unit cell; void space: 3206.384 Å^3 (83.32%) per unit cell

Reaction of CuBr with 1,3-Bis(phenylthio)propane in a 1:1 Ratio. Surprisingly, despite the rapidly growing number of MOFs, in which CuI SBUs are connected through acyclic dithioethers RS∩SR, there is almost no example of related CuBr-containing compounds. To the best of our knowledge, the only example of a crystallographically characterized CuBr coordination polymer assembled through an acyclic dithioethers is the polymer $[Cu(\mu_2\text{-}Br)_2Cu\{\mu\text{-}p\text{-}EtSCH_2C_6H_4C_6H_4CH_2SEt\text{-}p\}_2]_n$, in which two 2,2′-bis(ethylthiomethyl)biphenyl ligands span the dinuclear $Cu(\mu_2\text{-}Br)_2Cu$ SBUs giving rise to an infinite 1D ribbon (see below).[16a,21] The reactivity of CuX with diethyl sulfide was recently re-examined and demonstrated that the nature of the halide has a major impact on the architecture of the solid-state structure.[22,23] Whereas X-ray diffraction confirmed formation of the 1D coordination polymer $[(Et_2S)_3\{Cu_4(\mu_3\text{-}I)_4\}]_n$ consisting of infinite chain of sulfide-bridged closed-cubane Cu_4I_4 units, the $CuBr{\cdot}SEt_2$ adduct of composition $[(Cu_3Br_3)(SEt_2)_3]_n$ exhibited a quite unusual alternation of $Cu(\mu_2\text{-}Br)_2Cu$ rhomboids and tetranuclear open-cubane-like Cu_4Br_4 SBUs within the 1D chain.[22]

This paucity of the structural information prompted us to extend our investigation on dithioether-assembled polymers of copper(I) bromide. The self-assembly reaction of CuBr with bis(phenylthio)propane in a 1:1 ratio was studied and huge brownish crystals of $[\{Cu(\mu_2\text{-}Br)_2Cu\}\{\mu\text{-}PhS(CH_2)_3SPh\}_2]_n{\cdot}0.5$ $PhS(CH_2)_3SPh$ (**3**) containing a half molecule of the free ligand were isolated in 43% yield from a cold concentrated MeCN solution. Because of the propensity of CuBr to oxidize slowly to Cu(II), a solution or wet crystals of **3** turned progressively to dark-green upon exposure to air. Therefore, handling under an argon atmosphere was needed. However, once dried, crystals of **3** and CuBr-containing polymers **6** and **9** did not deteriorate even for several days in contact with air. Crystallographic examination

dx.doi.org/10.1021/ic301385u | Inorg. Chem. 2012, 51, 9917−9934

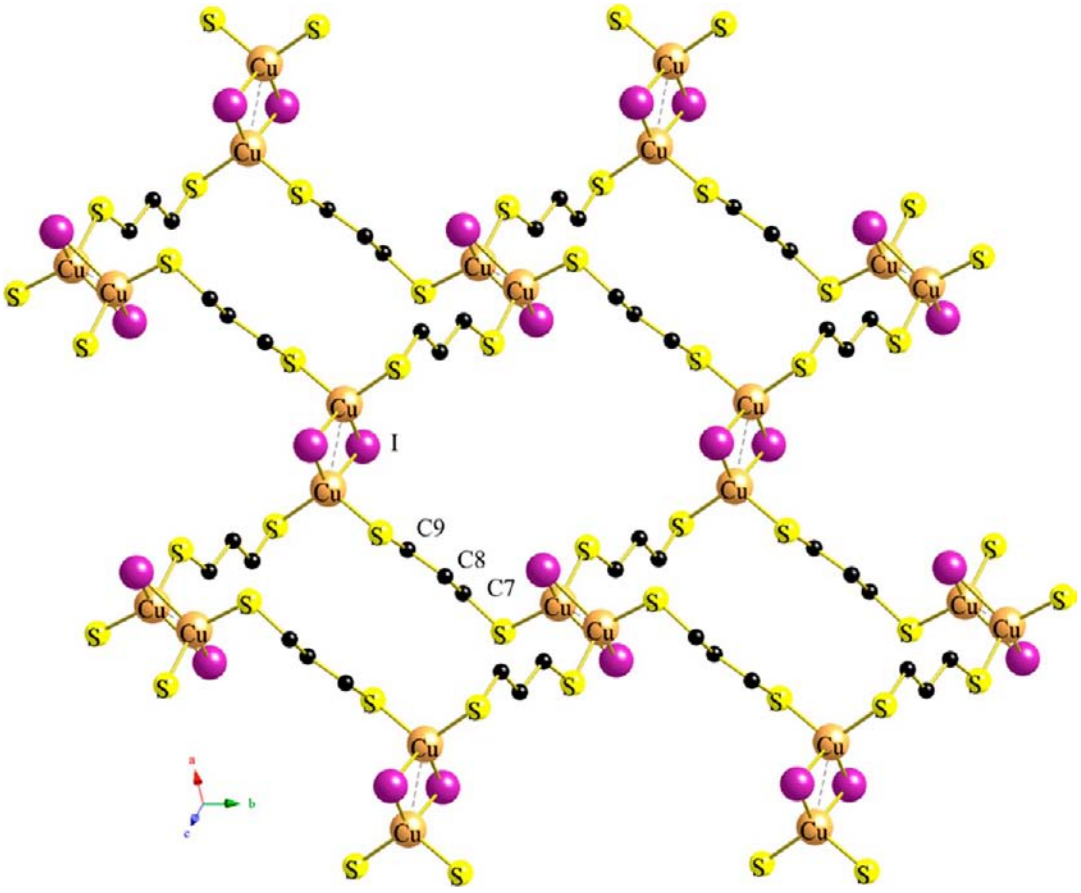

Figure 1. View on the *ab* plane of the 2D network of **1**. H atoms and phenyl groups are omitted for clarity. Selected bond lengths [Å] and angles [deg]: Cu−S(1) 2.332(2), Cu−S(2) 2.361(2), Cu−I 2.6521(12), Cu−I# 2.6403(12), Cu−Cu# 2.826(10); S(1)−Cu−S(2) 110.95(8), S(1)−Cu−I 105.30(6), S(1)−Cu−I# 117.39(7), S(2)−Cu−I# 102.17(7), S(2)−Cu−I 104.95(7), I#−Cu−I 115.46(4), Cu−I−Cu# 64.54(4), Cu−S(1)−C(1) 112.1(3). Symmetry transformations used to generate equivalent atoms: #1 $-x+1/2, y+1/2, z$; #2 $-x, -y+1, -z$; #3 $-x+1/2, y-1/2, z$.

of this 1D material revealed that dinuclear $Cu(\mu_2\text{-}Br)_2Cu$ units act as SBUs (Figure 3) like in $[Cu(\mu_2\text{-}Br)_2Cu\{\mu\text{-}p\text{-}EtSCH_2C_6H_4\text{-}C_6H_4CH_2SEt\text{-}p\}_2]_n$[16a] and the polymers below $[\{Cu(\mu_2\text{-}Br)_2Cu\}\{\mu\text{-}PhS(CH_2)_5SPh\}_2]_n$ (**6**) and $[\{Cu(\mu_2\text{-}Br)_2Cu\}_2\{\mu\text{-}p\text{-}TolS(CH_2)_5STol\text{-}p\}]_n$ (**9**). Concurrently, the three latter polymers exhibit Cu···Cu separations ranging between 2.9190(3) and 3.0345(10) Å, that are noticeably longer than that found in polymer **3**, which has a mean Cu···Cu distance of only 2.7851(12) Å at the limit of the van der Waals radii between two copper atoms.

Reaction of CuI with 1,5-Bis(phenylthio)pentane. Upon treatment of CuI with 1,5-bis(phenylthio)pentane in acetonitrile solution, the architecture of the resulting MOF depends on the metal-to-ligand ratio employed, again in a crucial manner. Performing the reaction in a 2:1 molar ratio gives air-stable crystals of general formula $[Cu_4I_4\{\mu\text{-}PhS(CH_2)_5SPh\}_2]_n\cdot PhS(CH_2)_5SPh$ (**4**) (Scheme 2). A first indication for the presence of Cu_4I_4 cubane clusters in the polymer came from the observation of the strong luminescence upon irradiation with UV-light at 366 nm (i.e., UV lamp). Indeed, an X-ray diffraction study confirms the incorporation of Cu_4I_4 cubane-type SBUs in a 1D polymeric structure. One disorderd bis(phenylthio)pentane molecule cocrystallizes per $[Cu_4I_4\{\mu\text{-}PhS(CH_2)_5SPh\}_2]$ unit within the molecular cell. In contrast to the 2D frameworks found for $[Cu_4I_4\{\mu\text{-}PhS(CH_2)_3SPh\}_2]$ (**2**) and $[Cu_4I_4\{\mu\text{-}PhS(CH_2)_4SPh\}_2]$, the Cu_4I_4 units are embedded inside an infinite 1D chain in polymer **4**, in which two ligands link the tetranuclear cores. The adjacent macrocycle is placed in an orthogonal arrangement with respect to the first one (Figure 5). Within the cluster core, the Cu−I bond lengths range between 2.6391(12) and 2.7745(14) Å. The $Cu_4(\mu_3\text{-}I)_4$ core of **4** is less distorted than that of **2** (Figure 4 **B**) since two Cu atoms are being related by symmetry. The Cu···Cu distances between the four Cu(I) centers [2.643(3)−2.757(3) Å] fall below the sum of the van der Waals radii (2.8 Å). At 193 K, the mean Cu···Cu separations compare to that of **2** (2.713 vs 2.727 Å, regardless of the different temperatures). The values are somewhat superior to those for the 1D polymer $[Cu_4I_4\{\mu\text{-}PhS_2CH_2SPh\}_2]_n$ (2.678 Å) and 2D polymer $[Cu_4I_4\{\mu\text{-}PhS_2(CH_2)_4SPh\}_2]_n$ (2.694 Å).[12] For the recently reported metalla-macrocycle $[Cu_4I_4(MeCN)_2\{\mu\text{-}bis\text{-}(2,4\text{-}Me_2C_6H_3S_2CH_2SC_6H_3Me_2\text{-}2,4\}]_2$ bridged by the bulky ligand bis(2,4-dimethylphenylthio)methane, an averaged Cu···Cu distance of 2.690(1) Å (at 100 K) has been detemined.[24] For a few Cu_4I_4-containing MOFs assembled by aliphatic dithioethers, the mean Cu···Cu separations are slightly longer than those found for polymer **4**. These examples include the 2D $[Cu_4I_4\{\mu\text{-}EtS(CH_2)_4SEt\}_2]_n$ (2.75 Å at 293 K) and 3D $[Cu_4I_4\{\mu\text{-}BzS(CH_2)_4SBz\}_2]_n$ (2.81 Å at 293 K), and 2D $[Cu_4I_4\{\mu\text{-}n\text{-}BuS(CH_2)_4SBu\text{-}n\}_2]_n$ polymers (2.7265(10) Å at 115 K), respectively.[14d,25] Another example is the (4,4)-connected 2D polymer $[(Cu_4I_4)\{\mu\text{-}4,4'\text{-}bis(ethylthiomethyl)biphenyl)_{1.5}(H_2O)]$ [2.814(16) Å at 291 K].[14e] For 2D polymer $[Cu_4I_4\{\mu\text{-}t\text{-}BuS\text{-}(CH_2)_4SBu\text{-}t\}_2]_n$ linked by the bulky *t*-$BuS(CH_2)_4SBu$-*t* ligand, even 2.911(2) Å have been evidenced at 115 K.[25]

dx.doi.org/10.1021/ic301385u | *Inorg. Chem.* 2012, 51, 9917−9934

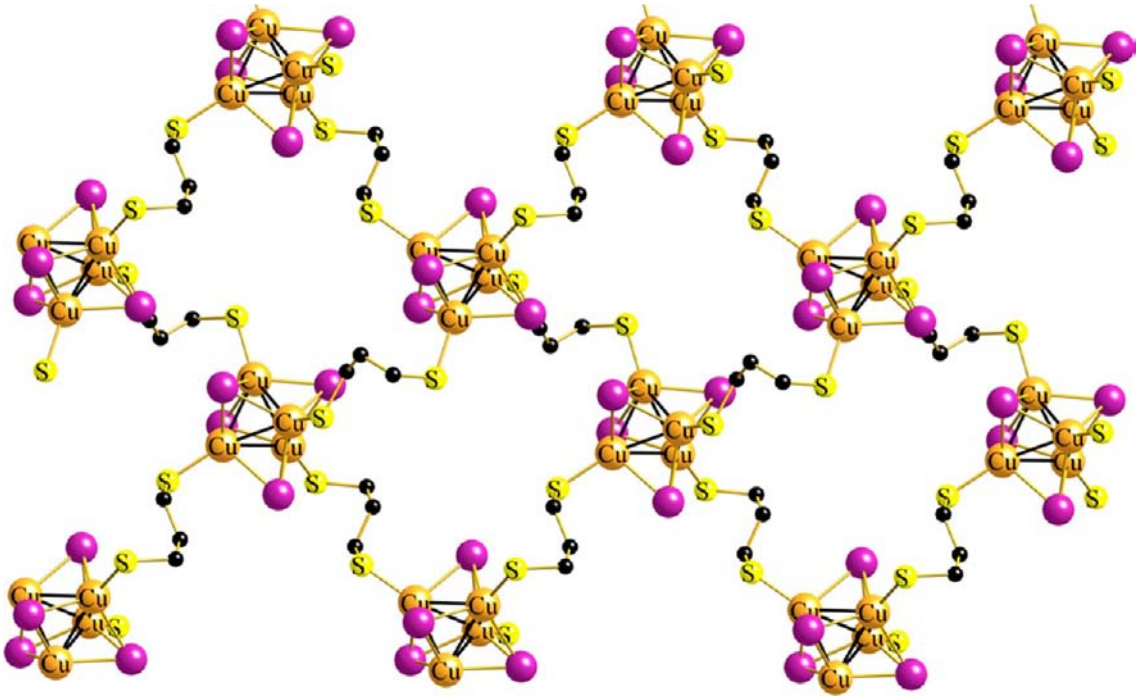

Figure 2. View on the *ab* plane of the 2D network of **2**. H atoms and phenyl groups are omitted for clarity. Selected bond lengths [Å]: Cu(1)−S(1) 2.300(17), Cu(2)−S(2) 2.3032(16), Cu(3)−S(3) 2.3122(17), Cu(4)−S(4) 2.3296(17), Cu(1)−Cu(2) 2.7047(12), Cu(1)−Cu(3) 2.7042(12), Cu(1)−Cu(4) 2.7675(12), Cu(2)−Cu(3) 2.7041(13), Cu(2)−Cu(4) 2.7556(13), Cu(3)−Cu(4) 2.7269(12), Cu(1)−I(1) 2.6011(11), Cu(1)−I(2) 2.7813(10), Cu(1)−I(3) 2.6640(13), Cu(2)−I(1) 2.7039(10), Cu(2)−I(2) 2.6553(10), Cu(2)−I(4) 2.6761(10), Cu(3)−I(1) 2.6966(11), Cu(3)−I(3) 2.6729(10), Cu(3)−I(4) 2.6692(10) Cu(4)−I(2) 2.6874(12), Cu(4)−I(3) 2.7076(10), Cu(3)−I(4) 2.6586(10); Symmetry transformations used to generate equivalent atoms: #1 $-x$, $y+1/2$, $-z+3/2$; #2 $-x$, $-y-1/2$, $-z+3/2$; #3 $-x-1$, $y+1/2$, $-z+3/2$; #4 $-x-1$, $y-1$, $-z+3/2$.

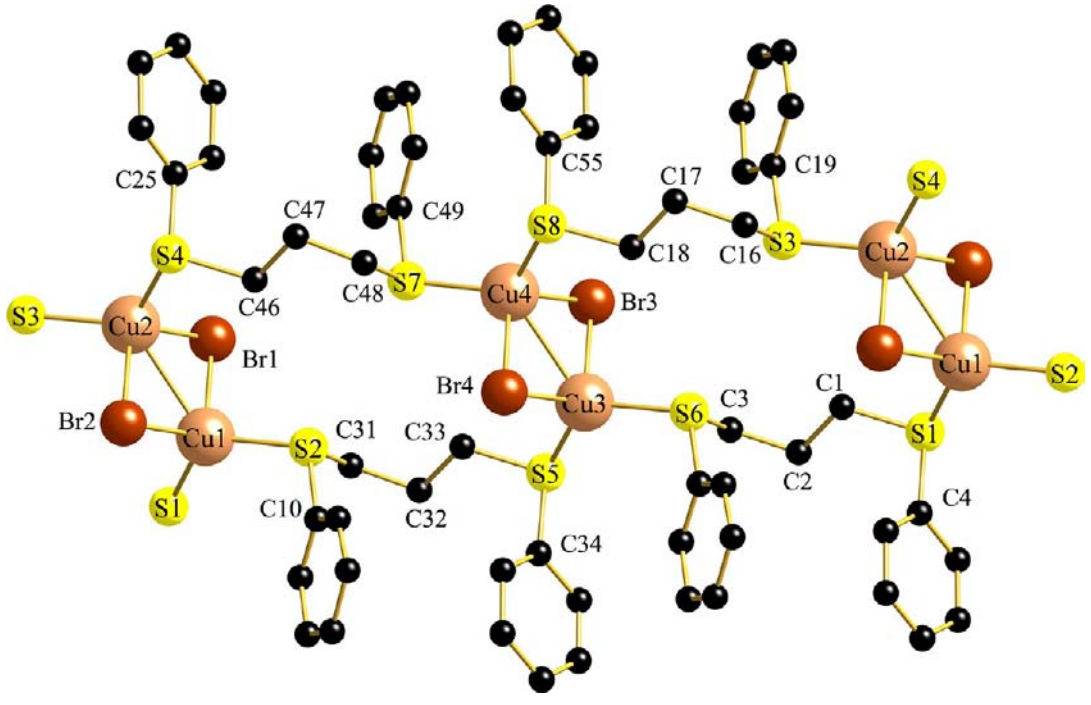

Figure 3. View of the infinite ribbon of **3** incorporating dinuclear $Cu(\mu_2\text{-}Br)_2Cu$ motifs. Selected bond lengths [Å] and angles [deg]: Cu(1)−S(1) 2.339(4), Cu(1)−S(2) 2.286(3), Cu(2)−S(3) 2.283(3), Cu(2)−S(4) 2.342(4), Cu(3)−S(5) 2.338(4), Cu(3)−S(6) 2.291(3), Cu(4)−S(7) 2.291(3), Cu(4)−S(8) 2.339(4), Cu(1)−Br(1) 2.537(2), Cu(1)−Br(2) 2.450(2), Cu(2)−Br(1) 2.437(2), Cu(2)−Br(2) 2.558(2), Cu(3)−Br(3) 2.538(2), Cu(3)−Br(4) 2.434(2), Cu(4)−Br(3) 2.456(2), Cu(4)−Br(4) 2.533(2), Cu(1)···Cu(2) 2.7941(11), Cu(3)···Cu(4) 2.7761(12); S(1)−Cu(1)−S(2) 118.96(14), S(3)−Cu(2)−S(4) 118.82(14), S(5)−Cu(2)−S(6) 119.07(14), S(7)−Cu(2)−S(8) 119.82(14), Br(1)−Cu(1)−Br(2) 112.08(8), Br(1)−Cu(2)−Br(2) 111.80(8), Br(3)−Cu(3)−Br(4) 112.57(8), Br(3)−Cu(4)−Br(4) 111.97(8), Cu(1)−Br(1)−Cu(2) 68.33(6), Cu(1)−Br(2)−Cu(2) 67.79(6), Cu(3)−Br(3)−Cu(4) 67.53(6), Cu(3)−Br(4)−Cu(4) 67.93(6). Symmetry transformations used to generate equivalent atoms: #1 $x+1$, y, $z+1$; #2 $x-1$, y, $-z-1$.

dx.doi.org/10.1021/ic301385u | *Inorg. Chem.* 2012, 51, 9917−9934

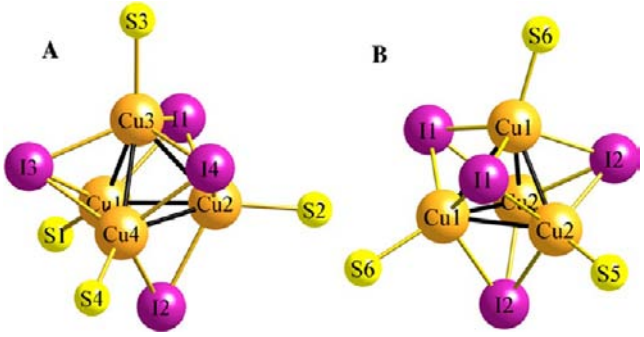

Figure 4. Comparison of the local symmetry of closed cubane-type $Cu_4(\mu_3\text{-}I)_4$ cores of 2D polymer **2** (**A**) and 1D polymer **4** (**B**).

The self-assembly reaction of CuI with bis(phenylthio)-pentane in a 1:1 ratio was also examined to address the influence of the metal-to-ligand ratio on the composition of the material. Indeed, elemental analyses of the colorless crystals isolated from a concentrated MeCN solution were consistent with the ligation of one dithioether ligand per copper center. The crystallographic analysis of this material of composition $[\{Cu(\mu_2\text{-}I)_2Cu\}\{\mu\text{-}PhS(CH_2)_5SPh\}_2]_n$ (**5**) revealed the presence of infinite 1D ribbons. These corrugated ribbons are built with two bridging dithioether ligands bridging a rhomboid Cu_2I_2 SBU. Each copper center of these nodal Cu_2I_2 units is coordinated in a tetrahedral manner by two S atoms stemming from two different dithioether ligands and is symmetrically bridged by two μ-iodine ligands. Twenty-membered macrocycles comprising 10 carbon atoms, 4 copper atoms, 4 sulfur atoms, and 2 μ-I atoms result from this arrangement and are annulated along the *a* axis (Figure 6).

The mean Cu−S distance of the two copper−thioether bonds of 1D polymer **5** is quite similar to the value found for the 2D polymer **1** (2.3325 vs 2.346 Å), but notably longer than the mean Cu−S distance found in the 1D compound **4** (2.299 Å). The same trend was previously observed for $[\{Cu(\mu_2\text{-}I)_2Cu\}_2\{\mu\text{-}PhS(CH_2)_2SPh\}_2]_n$ and $[Cu_4I_4\{\mu\text{-}PhS_2CH_2SPh\}_2]_n$ where the averaged Cu−S bonds are 2.3427 and 2.2965 Å, respectively.

Noteworthy, the Cu···Cu separation is 3.0089(15) Å, which is considerably longer than that for polymer **1**. A similar architecture has been obtained by Kim et al. for the nonemissive 1D polymer $[\{Cu(\mu_2\text{-}I)_2Cu\}\{\mu\text{-}C_6H_{11}CH_2SCH_2C(=O)\text{-}NC_4H_8S\}_2]_n$, formed by the self-assembly of CuI with the carbonyl-functionalized dithioether 2-(cyclohexythio)-1-thio-morpholino-ethanone ligand.[26] Similarly to polymer **5**, the rhomboid Cu_2I_2 units exhibit loose Cu···Cu contacts of 2.98 Å within the unidimensional loop chain and act as connecting nodes. Although these distances are significantly beyond the sum the van der Waals radii of two copper atoms (2.8 Å), a much longer Cu···Cu separation of 3.18 Å has been reported for the 2D polymer $([Cu_2I_2(dtpcp)_2]\cdot thf)_n$ (dtpcp = 2,11-dithia[3.3]-paracyclophane).[27] This wide range of experimentally observed Cu···Cu separations in dinuclear Cu_2I_2 units ligated by thioether ligands indicates a certain degree of structural flexibility, which in combination of the intrinsic flexibility of the dithioether ligands, may account for the richness of structural motifs found in the solid-state structures of these compounds. In line with the elongation of the Cu···Cu distance, the Cu−I−Cu angle of **5** is

Scheme 2

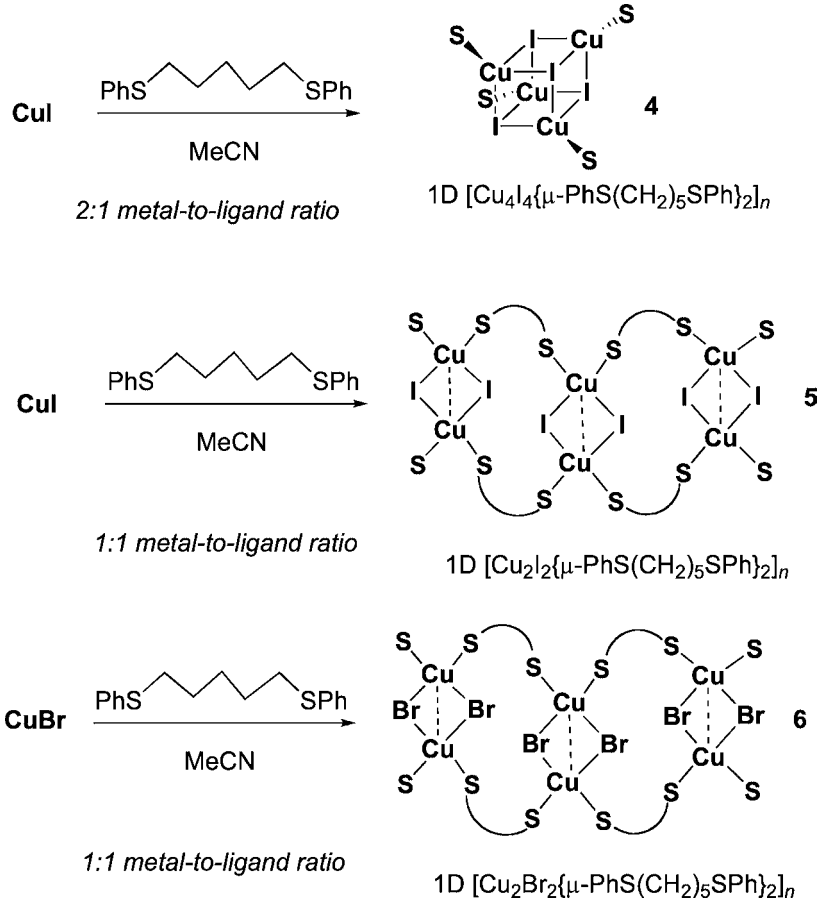

dx.doi.org/10.1021/ic301385u | *Inorg. Chem.* 2012, 51, 9917−9934

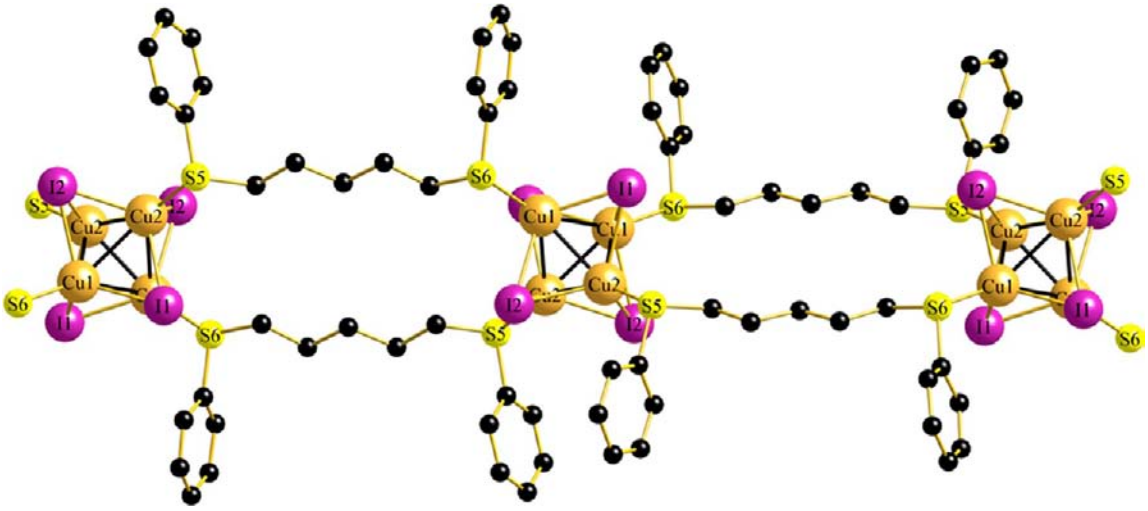

Figure 5. View on the 1D chain of **4** along the *a* axis. H atoms are omitted for clarity. Selected bond lengths [Å]: Cu(1)−S(6) 2.304(3), Cu(2)−S(5) 2.294(3), Cu(1)−Cu(2) 2.750(2), Cu(1)−Cu(1)#3 2.757(3), Cu(1)−Cu(2)#3 2.677(13), Cu(2)−Cu(2)#2 2.664(3), Cu(1)−I(1) 2.6958(17), Cu(1)−I(2) 2.7515(17), Cu(2)−I(2)#3 2.6453(19), Cu(2)−I(2) 2.6580(17), Cu(2)−I(1) 2.7803(17), I(1)−Cu(1)#3 2.6268(17); Symmetry transformations used to generate equivalent atoms: #1 $-x+1/2, -y+3/2, -z+1$; #2 $-x+1/2, -y+3/2, -z+2$; #3 $-x+1, y, -z+3/2$.

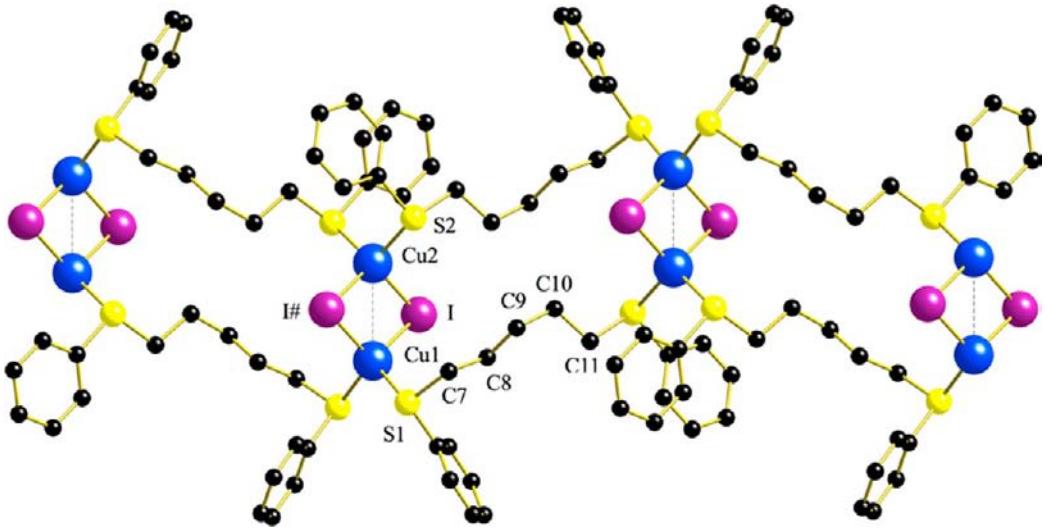

Figure 6. View of the ribbon of **5** incorporating dinuclear $Cu(\mu_2\text{-}I)_2Cu$ motifs along the *a* axis. Selected bond lengths [Å] and angles [deg]: Cu(1)−S(1) 2.3071(10), Cu(2)−S(2) 2.3580(11), Cu(1)−I 2.6337(8), Cu(1)−I# 2.6337(8), Cu(1)···Cu(2) 3.0089(15); S(1)−Cu−S(1)# 106.90(5), S(2)−Cu(2)−S(2)# 111.46(5), S(1)−Cu(1)−I 100.88(3), S(1)−Cu−I# 100.88(3), S(2)−Cu(2)−I 102.78(3), S(2)−Cu−I 102.78(3), I#−Cu(1)−I 110.60(4), I#−Cu(2)−I 110.23(4), Cu(1)−I−Cu(2) 69.58(3), Cu(1)−S(1)−C(1) 110.75(10). Symmetry transformations used to generate equivalent atoms: #1 $-x+3/2, -y+1/2, -z+2$; #2 $-x+1, y, -z+3/2$.

markedly less acute than that of **1** [69.58(3) vs 64.54(4)°]. The Cu−I distances of **5** and **1** are less affected by this phenomenon and lie in the 2.63−2.65 Å range.

Reaction of CuBr with 1,5-Bis(phenylthio)pentane in a 1:1 Ratio. For comparison, an acetonitrile solution of bis(phenylthio)pentane was also treated with an equimolar amount of CuBr. At 5 °C, colorless crystals of composition $[\{Cu(\mu_2\text{-}Br)_2Cu\}_2\{\mu\text{-}PhS(CH_2)_5SPh\}_2]_n$ (**6**) were formed and isolated in 77% yield. Crystallographic analysis revealed that this compound, crystallizing in the monoclinic crystal system with space group *C*2/*c*, is isomorphous with $[\{Cu(\mu_2\text{-}I)_2Cu\}\{\mu\text{-}PhS(CH_2)_5SPh\}_2]_n$ (**5**). Indeed, the 1D scaffold of $[\{Cu(\mu_2\text{-}Br)_2Cu\}_2\{\mu\text{-}PhS(CH_2)_5SPh\}_2]_n$ (**6**) comprises in an identical manner dinuclear $Cu(\mu_2\text{-}Br)_2Cu$ rhomboids, which are linked by 2 bridging dithioethers (Figure 7). The Cu···Cu contact is somewhat shorter than that of its μ_2-iodide analogue [2.9190(3) vs 3.0089(15) Å], but both the Cu(1)−X−Cu(2) angles and Cu−S bond lengths of **5** and **6** lie in the same range.

The structural arrangement within the ribbon of polymer **6** is also comparable with that of the aforementioned compound $[Cu(\mu_2\text{-}Br)_2Cu\{\mu\text{-}p\text{-}EtSCH_2C_6H_4C_6H_4CH_2SEt\text{-}p\}_2]_n$,[16a] in which two 2,2′-bis(ethylthiomethyl)biphenyl ligands span dinuclear $Cu(\mu_2\text{-}Br)_2Cu$ SBUs giving rise to an infinite 1D strand as encountered in **6**. The Cu−Br bond lengths [2.499(1) and 2.536(1) Å] of the latter compound are quite similar to those of **6**, the separations between the metal centers [2.918 vs 2.9190(3) Å] are even almost identical.

Reaction of CuI with 1,5-Bis(p-tolylthio)pentane. The influence of the substitution pattern of the aryl group of the dithioether ligand on the composition and topology of the resulting MOF was also addressed and the reaction between 1,5-bis(*p*-tolylthio)pentane and CuI was examined (Scheme 3).

dx.doi.org/10.1021/ic301385u | *Inorg. Chem.* 2012, 51, 9917−9934

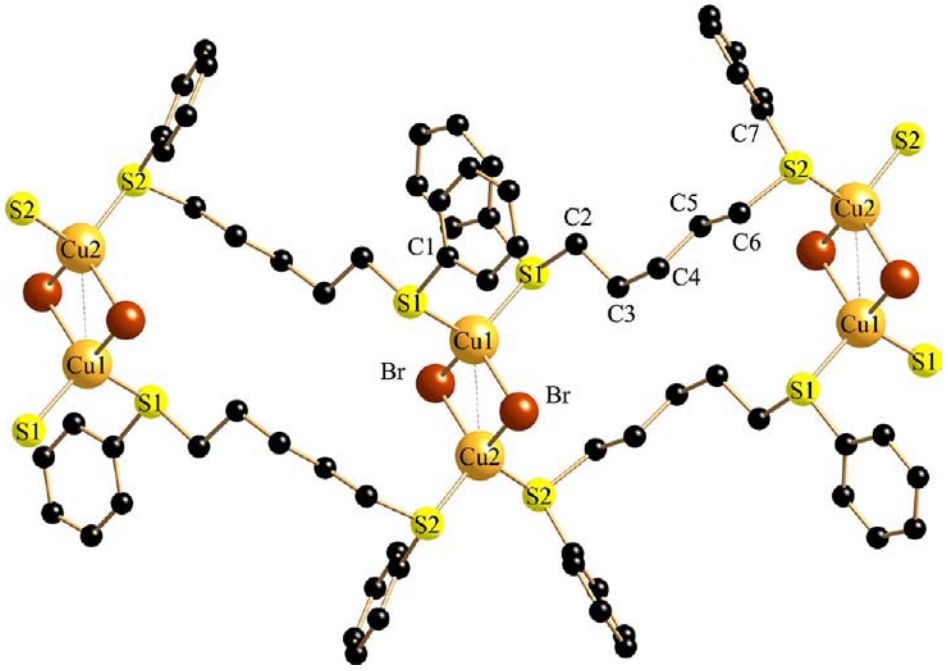

Figure 7. View of the infinite ribbon of **6** incorporating dinuclear Cu(μ_2-Br)$_2$Cu motifs. Selected bond lengths [Å] and angles [deg]: Cu(1)−S(1) 2.3294(2), Cu(2)−S(2) 2.2856(2), Cu(1)−Br 2.48812(17), Cu(2)−Br 2.49130(17), Cu(1)···Cu(2) 2.9190(3); S(1)−Cu−S(1)# 111.464(12), S(2)−Cu(2)−S(2)# 107.544(12), S(1)−Cu(1)−Br 103.287(7), S(1)−Cu(1)−Br# 115.437(6), S(2)−Cu(2)−Br 102.432(6), S(2)−Cu(2)−Br# 118.584(6), Br#−Cu(1)−Br 108.323(8), Br#−Cu(2)−Br 108.121(8), Cu(1)−Br−Cu(2) 71.778(7), Cu(1)−S(1)−C(1) 105.32 (3), Cu(2)−S(2)−C(7) 113.49(3). Symmetry transformations used to generate equivalent atoms: #1 *x*, *y*, *z*+3/2; #2 −*x*+1/2, −*y*+1/2, −*z*+2.

Scheme 3

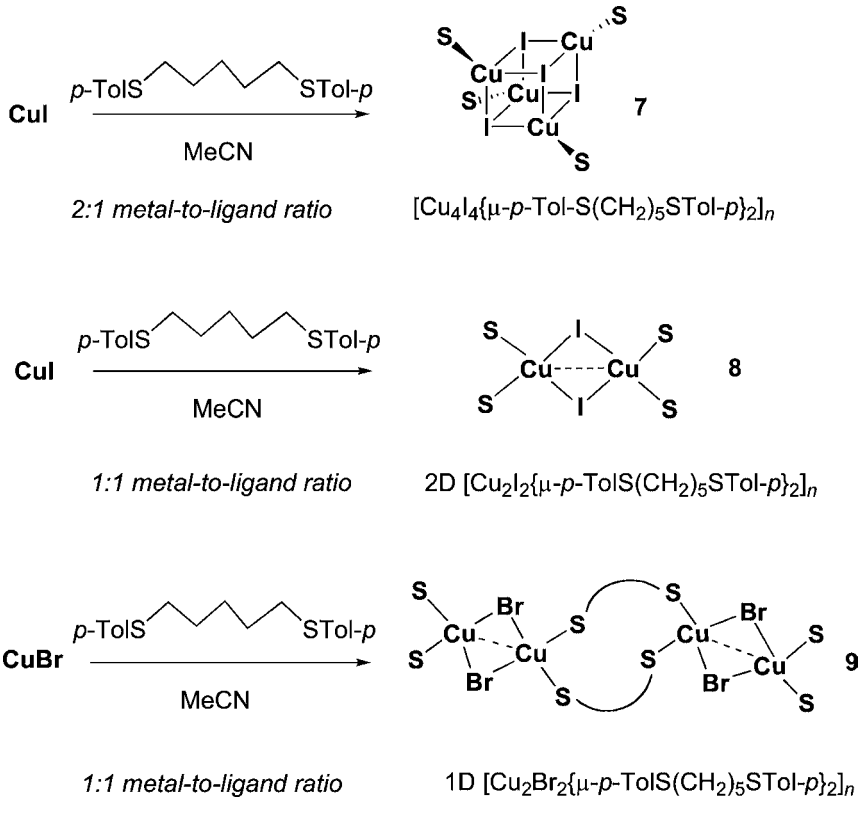

Unfortunately, no single-crystal of this colorless compound suitable for X-ray analysis was obtained. These crystals exhibit an intense green-yellow emission under UV-light at 366 nm indicating the presence of the Cu_4I_4 cluster, and the elemental analyses indicate formation of a MOF of unknown dimensionality but with the composition $[Cu_4I_4\{\mu\text{-pTolS}(CH_2)_5\text{STol-p}\}_2]_n$ (**7**). The clear demonstration for the presence of Cu_4I_4 SBUs is the very strong luminescence observed at ∼545 nm for polymer **7** at 298 K

dx.doi.org/10.1021/ic301385u | *Inorg. Chem.* 2012, 51, 9917−9934

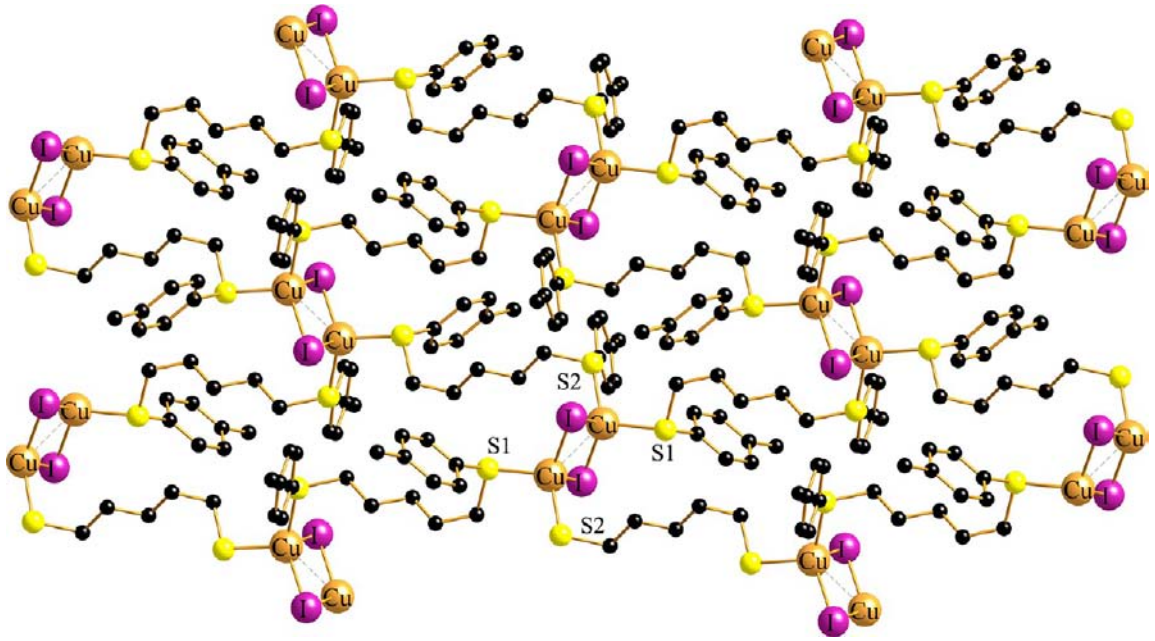

Figure 8. View of a layer of **8** incorporating dinuclear $Cu(\mu_2\text{-}I)_2Cu$ motifs. Selected bond lengths [Å] and angles [deg]: Cu−S(1) 2.3632(9), Cu−S(2) 2.3401(11), Cu−I 2.5942(6), Cu−I# 2.6742(6), Cu−Cu# 2.8549(10); S(1)−Cu−S(2) 109.59(4), S(1)−Cu−I 110.55(3), S(1)−Cu−I# 98.21(3), S(2)−Cu−I# 99.98(3), S(2)−Cu−I 121.33(3), I−Cu−I# 114.40(2), Cu−I−Cu# 65.60(2), Cu−S(1)−C(1) 113.74(13). Symmetry transformations used to generate equivalent atoms: #1 x, $-y+1/2$, $z-1/2$; #2 x, $-y+1/2$, $z+1/2$; #3 $-x$, $-y$, $-z+1$.

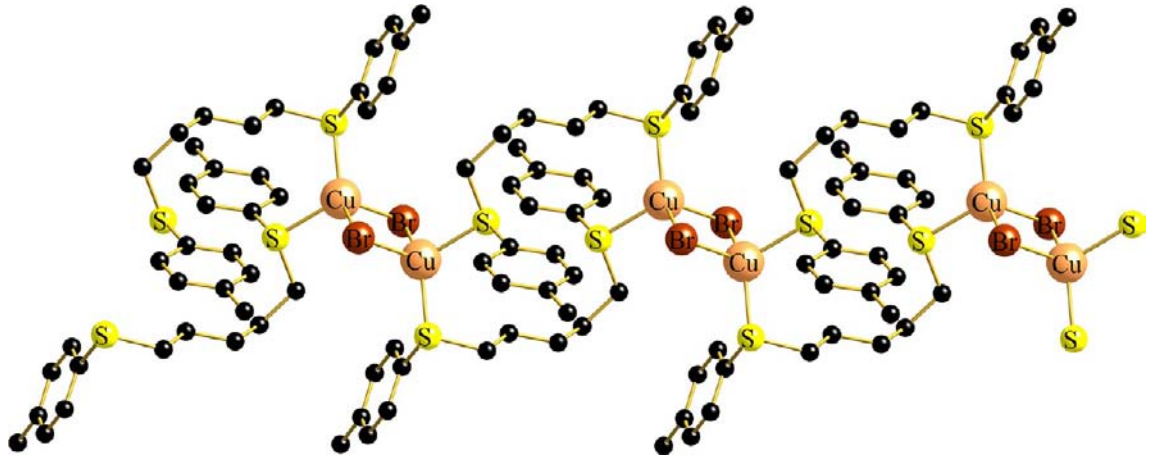

Figure 9. View of the ribbon of **9** incorporating dinuclear $Cu(\mu_2\text{-}Br)_2Cu$ motifs along the b axis. Selected bond lengths [Å] and angles [deg]: Cu−S(1) 2.2276(11), Cu−S(2) 2.3253(11), Cu−Br 2.4724(7), Cu−Br# 2.5362(8), Cu···Cu# 3.0345(10); S(1)−Cu−S(2) 112.62(4), S(1)−Cu−Br 124.53(4), S(1)−Cu−Br# 105.01(4), S(2)−Cu−Br 99.76(3), S(2)−Cu−Br# 108.70(3), Br−Cu−Br# 105.43(2) Cu−Br−Cu# 74.57(2), Cu−S(1)−C(1) 113.17(12), Cu−S(2)−C(13) 109.01(12). Symmetry transformations used to generate equivalent atoms: #1 $-x$, $-y$, $-z+2$; #2 $-x$, $-y+1$, $-z+2$.

(Supporting Information, Figures S4 and S5), which is distinctive of the weaker and more blue-shifted emission for the Cu_2I_2-containing polymers.

In the case of 1,5-bis(*p*-tolylthio)pentane, the composition of the MOF depends again on the metal-to-ligand ratio. A colorless 2D coordination polymer $[\{Cu(\mu_2\text{-}I)_2Cu\}\{\mu\text{-}p\text{-}TolS(CH_2)_5STol\text{-}p\}]_n$ (**8**) was isolated in 81% yield after mixing CuI with 1,5-bis(*p*-tolylthio)pentane in a 1:1 ratio. Indeed, single crystal analysis revealed that the substitution pattern of the -SAr ring (*p*-Tol vs Ph) has an impact on the dimensionality of the framework. In contrast to 1D polymer **5**, the network of **8** is constituted of 2D sheets incorporating centro-symmetric $Cu(\mu_2\text{-}I)_2Cu$ rhomboids as SBUs (Scheme 3 and Figure 8). Compared with the loose Cu···Cu contacts of polymer **5**, those of polymer **9** are much shorter and compare more favorably to those of **2** (2.8549(10) vs 2.826(10) Å, neglecting the different recording temperatures). Using the CrystalMaker Software (version 8.6.2), the porosity (corrected for first-nearest-neighbor sphere overlap and site visibility) of **8** has been calculated: filled space: 243.202 $Å^3$ (12.04%) per unit cell; void space: 1777.047 $Å^3$ (87.96%) per unit cell

Reaction of CuBr with 1,5-Bis(p-tolylthio)pentane in a 1:1 Ratio. To address the influence of the halide ligand on the network topology, 1,5-bis(*p*-tolylthio)pentane was reacted with CuBr in a 1:1 ratio in MeCN. An X-ray diffraction study revealed that the change in halide ion (Br^- vs I^-) causes a change in the dimensionality of the MOF (Scheme 3). A colorless material crystallizing in the triclinic crystal system, space group $P\bar{1}$, was isolated in 78% yield and identified as the 1D polymer $[\{Cu(\mu_2\text{-}Br)_2Cu\}_2\{\mu\text{-}p\text{-}TolS(CH_2)_5STol\text{-}p\}]_n$ (**9**), (Figure 9). At the first glance, polymer **9** resembles much more $[\{Cu(\mu_2\text{-}Br)_2Cu\}\{\mu\text{-}PhS(CH_2)_5SPh\}_2]_n$

dx.doi.org/10.1021/ic301385u | *Inorg. Chem.* 2012, 51, 9917−9934

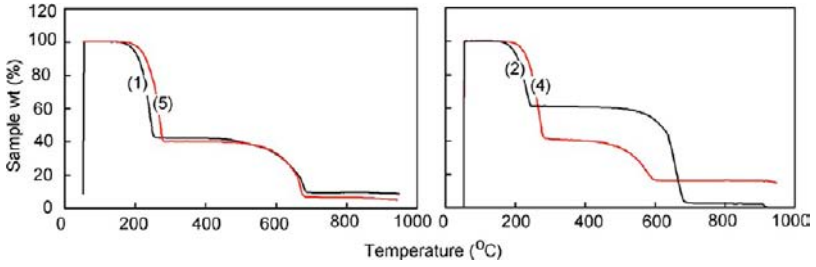

Figure 10. TGA traces for the CuI coordination polymers **1**, **2**, **4**, and **5**.

(**6**) than $[\{Cu(\mu_2\text{-}I)_2Cu\}\{\mu\text{-}p\text{-}TolS(CH_2)_5STol\text{-}p\}]_n$ (**8**). Like in the former polymer, the 1D ribbon comprises dinuclear $Cu(\mu_2\text{-}Br)_2Cu$ SBUs, which are spanned by the two dithioethers. The $Cu(\mu_2\text{-}Br)_2Cu$ core has a planar parallelogram geometry, where the two Cu(I) centers at the apexes are separated by 3.0345(10) Å (vs 2.9190(3) Å in **6**). The Cu−Br bond lengths are quite similar [2.4724(7) and 2.5362(8) Å], therefore the bridging by the μ_2-Br atoms can be considered approximately symmetric, with a Cu−Br−Cu angle of 74.57(2)°. However, in contrast to polymer **6**, where the $Cu(\mu_2\text{-}Br)_2Cu$ SBUs are orthogonal with respect to the propagation axis of the infinite chain, the $Cu(\mu_2\text{-}Br)_2Cu$ rhomboids of **9** are oriented in a diagonal manner forming 16-membered macrocycles instead of 20-membered ones.

Using the new crystallographic data of polymers **3**, **6**, and **9** exhibiting $Cu(\mu_2\text{-}Br)_2Cu$ cores, a comparison of their structural parameters with those of polymers **1**, **5**, and **8** with $Cu(\mu_2\text{-}I)_2Cu$ is appropriate. According Pearson's HSAB principle, I^- confers a softer character to a Cu(I) ion with respect to Br^-. Moreover CuBr is smaller than CuI and the Cu−Br bond is shorter than the Cu−I bond, which could be relevant for the metric parameters of the dinuclear $Cu(\mu_2\text{-}X)_2Cu$ motif. So a shorter Cu···Cu separation for $Cu(\mu_2\text{-}Br)_2Cu$ with respect to $Cu(\mu_2\text{-}I)_2Cu$ may expected. This trend is indeed noted when comparing the data for polymer **3**, $[\{Cu(\mu_2\text{-}Br)_2Cu\}\{\mu\text{-}PhS(CH_2)_3SPh\}_2]_n$) with those for **1**, $[\{Cu(\mu_2\text{-}I)_2Cu\}\{\mu\text{-}PhS(CH_2)_2SPh\}_2]_n$ [2.7851(12) vs 2.826(10) Å], which is also observed for the isomorphous polymers $[\{Cu(\mu_2\text{-}Br)_2Cu\}_2\{\mu\text{-}PhS(CH_2)_5SPh\}_2]_n$ (**6**) and $[\{Cu(\mu_2\text{-}I)_2Cu\}\{\mu\text{-}PhS(CH_2)_5SPh\}_2]_n$ (**5**) [2.9190(3) vs 3.0089(15) Å]. However, the $Cu(\mu_2\text{-}I)_2Cu$ distance in polymer **8** is significantly shorter than the looser $Cu(\mu_2\text{-}Br)_2Cu$ separation in **9** [2.826(10) vs 3.0345(10) Å]. So no clear tendency is yet obvious and more comparative data are necessary.

Thermal Stability of the Coordination Polymers. The thermal gravimetric analysis (TGA) traces of polymers **1**, **2**, **4**, and **5** exhibit two plateaus (Figure 10). The first one spreads from room temperature all the way to about 200 °C, and the second from about 250 to about 600 °C or above. On the basis of the difference in relative mass losses (in %) the decomposition is not associated with a simple loss of ligands, but rather with ligand decomposition. This is particularly evident when the residual mass of the materials at 800 °C or above corresponds to less than 10% of the total mass (even ∼0% for polymer **2**) strongly suggesting the formation of organometallic volatiles. The comparison of traces for **1** and **5** and for **2** with **4** (i.e., $-(CH_2)_3-$ vs $-(CH_2)_5-$) indicates clearly that the $-(CH_2)_5-$containing materials are more stable by about 30 °C than that for those containing the $-(CH_2)_3-$ chains. Perhaps a possible explanation is that the longer flexible chain $-(CH_2)_5-$ dissipates this thermal energy under the form of low-frequency molecular motions within this chain. The comparison of the traces for **1** and **2** (2D polymers) and **4** and **5** (1D polymers) indicates that the position of the second plateau in % mass losses and in thermal decomposition temperature is also dependent on the nature of the cluster (Cu_2I_2 vs Cu_4I_4) but no clear trend is noted. This observation can easily be explained by the likely different decomposition patterns of the $-(CH_2)_3-$ vs $-(CH_2)_5-$containing ligands prior to the formation of the decomposition materials of the second plateau.

The three Cu_2Br_2-containing polymers were also compared allowing the comparison of the thermal stability between Cu_2Br_2 vs Cu_2I_2, $-(CH_2)_3-$ vs $-(CH_2)_5-$, and Ph vs *p*-Tol (Figure 11).

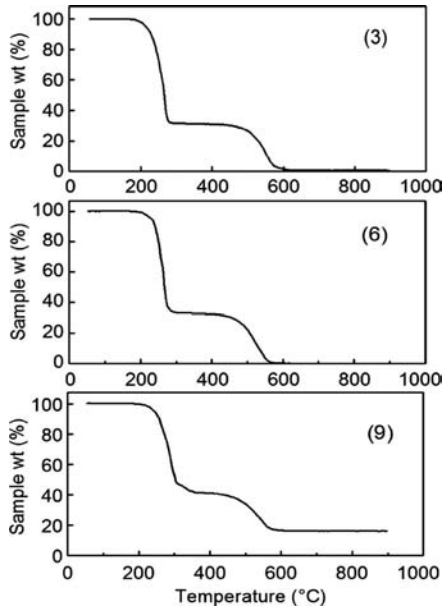

Figure 11. TGA traces for the CuBr coordination polymers **3**, **6**, and **9**.

The comparison between the traces for **1** and **3**, and **5** and **6** indicate a decrease of about 20° and 2−3° in decomposition temperatures going from Cu_2Br_2 to Cu_2I_2. This observation is in line with the above conclusion stating that the decomposition temperature is cluster-dependent. The comparison of the traces between **3** and **6** shows a slight increase of a few degres of the first weigth loss temperature, which is also in line with the better thermal stability of $-(CH_2)_5-$containing polymers. Finally, the comparison of **6** and **9** leads to the conclusion that the *p*-tolyl-containing polymer is more stable by about 10° than that for the Ph. Furthermore, there are cases where the formation of volatiles is noticed for polymers **3** and **5** where no residual is observed at temperatures exceeding 600 °C.

Steady State Luminescence Spectroscopy. The solid state absorption spectra (measured by reflectance spectroscopy) were examined for the $(CuI)_n$-containing coordination polymers (n = 1, 2) **1**, **2**, **4**, **5**, and **8** (Figure 12). Although the overall

dx.doi.org/10.1021/ic301385u | *Inorg. Chem.* 2012, 51, 9917−9934

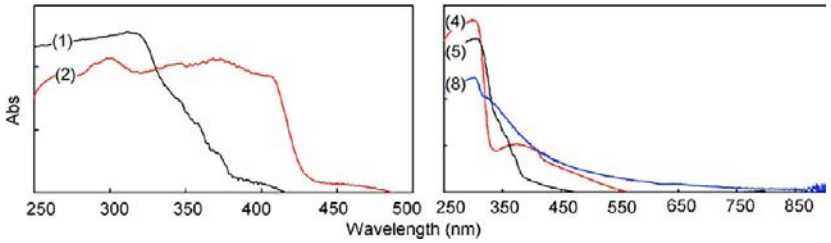

Figure 12. Solid-state absorption spectra of polymers **1**, **2**, **4**, **5**, and **8** at 298 K obtained from reflectance spectroscopy.

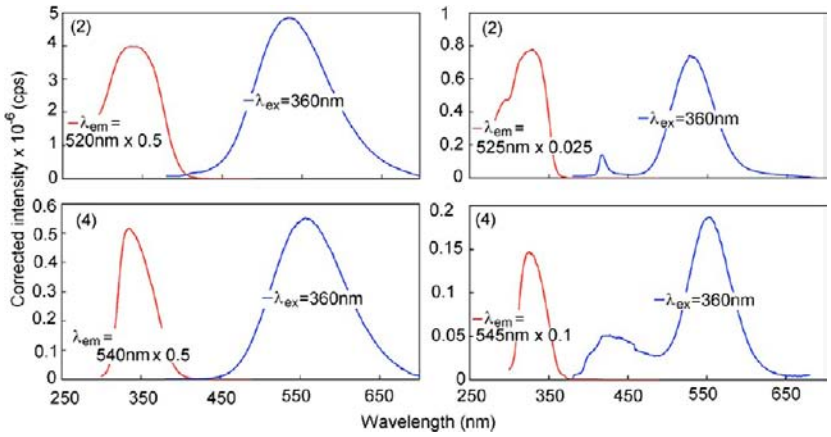

Figure 13. Solid state excitation (red) and emission (blue) of polymers **2** and **4** measured at 298 K (left) and 77 K (right).

shapes of the absorption spectra share similar features, the cubane (Cu_4I_4)-containing polymers **2** and **4** exhibit red-shifted bands above 350 nm. This relative position of the absorption signals is in line with the position of their respective luminescence below.

The presence of aryl-chromophores onto the dithioether ligands implies that the strong absorption band below 300 nm may include the $\pi-\pi^*$ transitions of the ligand as one of the components. The longer wavelength shoulder absorption observed for the cubane (Cu_4I_4)-containing polymers **2** and **4** can be assigned to cluster-centered transition (*CC*; major) mixed with halogen-to-ligand charge transfer (XLCT; minor) as previously reported for other analogous materials based on ab initio calculations.[28,29]

The solid state emission spectra for these cubane (Cu_4I_4)-containing polymers (**2** and **4**) exhibit the anticipated strong band located in the 500−600 nm spectral window similar to other related cubane-containing materials.[13a] Upon cooling the solid to 77 K, the red-shifted emission bands become narrower but do not greatly shift (the maxima remain the same at ±5 nm) but weaker signals appear in the blue region of the spectra at ∼400 nm. These features are also known for other related cubane-type cluster and arise from cluster-centered excited states.[28] The comparison of the emission maxima between **2** and **4** reveals a more red-shifted band for the -$(CH_2)_5$-containing polymer **4**. The average Cu···Cu and Cu−S distances in the cubane structures of polymers **2** and **4** are 2.727 and 2.311 Å and 2.711 and 2.300 Å, respectively. The shorter Cu···Cu and Cu−S distances in polymer **4** and the longer wavelength of the emission maximum comparatively to polymer **2** are perfectly consistent with the *CC* nature of the luminescent excited states.

Polymers **1** and **5** containing the Cu_2I_2 rhomboid motif exhibit very different luminescence properties. First, the emission intensities are somewhat weaker than that of the cubane analogues easily noticeable with naked eyes. Second, the recorded luminescence spectra exhibit emission maxima around 450 nm with variable vibronic components (Figure 14). The vibronic features are better resolved for polymer **1** than that for polymer **5**, likely reflecting the lesser number of CH_2 units in the flexible chain of the dithioether ligand. Except for an improvement of the resolution of the vibronic features, no new emission is depicted upon cooling the samples down to 77 K. The nature of the emissive excited states in these Cu_2I_2-containing polymers is expected to be different from those arising from the cubanes due the difference in their band shapes. The nature of the excited state for the motif $Cu_2I_2L_4$ (L = pyridine) was also previously worked out by Ford and his co-workers using theoretical calculations (ab initio).[28] The conclusion was that the lowest energy excited states are a mixture 54:40% of cluster-centered and XLCT (halide-to-ligand charge transfer), which resembles that for $Cu_4I_4(pyridine)_4$ analogue.

Polymer **8** exhibits a more complicated behavior (Figure 14). The luminescence spectra exhibit a very large emission band spreading from 350 to 650 nm where two components are suspected at 298 K. Upon cooling the solid samples to 77 K, some vibronic features appear, but the resolution of the two bands (if any) was not observed. On the basis of the above X-ray crystallographic and luminescence studies, any (Cu_2I_2)-containing materials should exhibit an emission centered at 450 nm, and any (Cu_4I_4)-containing polymers should display an emission in the 500−600 nm range. For polymer **8**, both ranges are apparent, and we come to the conclusion that this investigated material includes both types of clusters, presumably small amounts of polymer **7**. This is confirmed below. Knowing that the Cu_4I_4-species are strongly luminescent, this contamination appears small but clearly visible. Their separation was not successful.

The $Cu_2Br_2S_4$-containing polymers **3**, **6**, and **9** were also investigated despite their very low intensity of emission (Figures 15 and 16). While the polymers are weakly or not luminescent at 298 K, these materials are all weakly emissive at 77 K. To the best

dx.doi.org/10.1021/ic301385u | *Inorg. Chem.* 2012, 51, 9917−9934

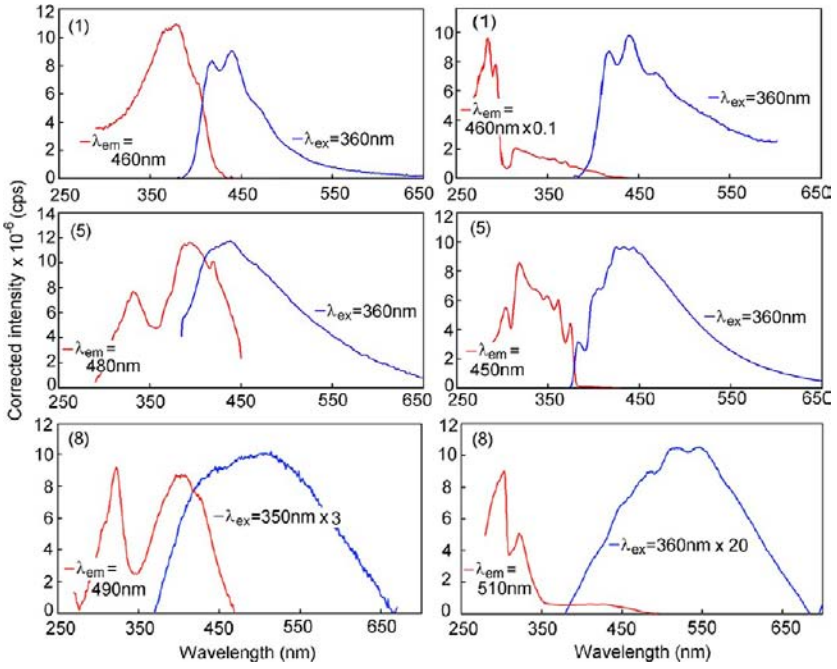

Figure 14. Solid state excitation (red) and emission (blue) of polymers **1**, **5**, and **8** at 298 (left) and 77 K (right).

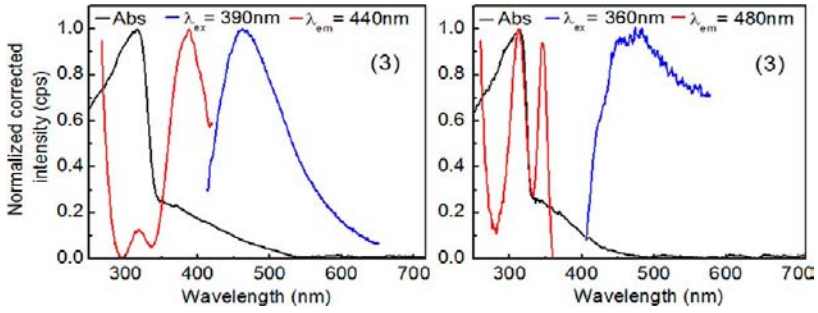

Figure 15. Solid state absorption (black), excitation (red), and emission (blue) of polymer **3** measured at 298 K (left) and 77 K (right).

of our knowledge, this is the first report of luminescence arising from the Cu_2Br_2-containing unit. Qualitatively, the relative emission intensities of these polymers vary as $Cu_4I_4 > Cu_2I_2 > Cu_2Br_2$. This trend is consistent with the relative emission lifetimes presented below.

Time-Resolved Spectroscopy and Photophysical Study. The emission lifetimes for polymers **1**, **2**, **4**–**6**, **8** and **9** are shown in Table 3. Three distinctive trends are noted. First, the short wavelength bands placed below 500 nm (i.e., arising from the Cu_2I_2 species; polymers **1** and **5**) exhibit a shorter luminescence lifetimes (<1.4 μs) than that for the Cu_4I_4 cubane-containing polymers. Second, the emission lifetimes of the weakly emissive Cu_2Br_2 species are also found to be very short-lived (ns time scale). Finally, the increase in lifetimes upon cooling the samples is also observed, which is consistent with the increase in rigidity of the materials (i.e., decrease in the non-radiative rate constants).

The long wavelength bands placed above 500 nm arising from the Cu_4I_4 clusters (polymers **2** and **4**) exhibit lifetimes >1.0 μs at 298 K that increases upon cooling to 77 K up to 6 and 8 μs for **2** and **4**, respectively. These same polymers also exhibit shorter wavelength bands below 500 nm at 77 K (Figure 13), and their corresponding lifetimes are also short (~0.6 μs). These short and long-lived components have also been well observed in the time-resolved spectra for polymer **2** as a representative example (the short wavelength band decays more rapidly that the long one). Similarly, time-resolved spectra for polymer **5** (as a representative example) exhibit only one signal at 450 nm and one shorter lifetime (Figure 17). The two emission lifetimes of 0.6 (λ_{max} = 420 nm) and 6–8 μs (540 ± 15 nm) differ from that reported for the strongly luminescent cubane-containing polymers $[Cu_4I_4\{\mu\text{-}RS(CH_2)_4SR\}_2]_n$ (R = *n*-Bu, *t*-Bu (averaging λ_{max} = 400 nm, τ_e = 100 ± 2 μs and λ_{max} = 545 ± 5 nm, τ_e = 4–6 μs at 77 K), notably for the short wavelength emission.[25] Conversely, these lifetimes are perfectly in line with those reported for the polymer $[Cu_4I_4\{\mu\text{-}PhS(CH_2)_4SPh\}_2]_n$ (λ_{max} = 430 nm, τ_e = 0.60 ± 0.02 μs; λ_{max} = 600 nm, τ_e = 3.36 ± 0.01 μs at 77 K).[12b] This observation suggests that the low-energy emission is R-dependent (alkyl vs aryl).

The emission data for polymers **1** and **5** (Cu_2I_2-containing polymers) are found in the 0.6–1.4 μs time scale at 298 and 77 K, and are relatively weakly temperature-dependent. These data compare with those reported for the S–S bonded *cyclo*-1,2-dithian-containing polymer $[Cu_2I_2\{S(CH_2)_4S\}]_n$ (T = 298 K: λ_{max} = 378 nm, τ_e = 1.04 ± 0.01 μs and λ_{max} = 535 nm, τ_e = 0.97 ± 0.04 μs; T = 77 K: λ_{max} = 413 nm, τ_e = 1.43 ± 0.02 μs and λ_{max} = 640 nm, τ_e = 1.49 ± 0.04 μs), but are slightly shorter. This small difference is certainly related to the rigidity of the polymer

dx.doi.org/10.1021/ic301385u | *Inorg. Chem.* 2012, 51, 9917–9934

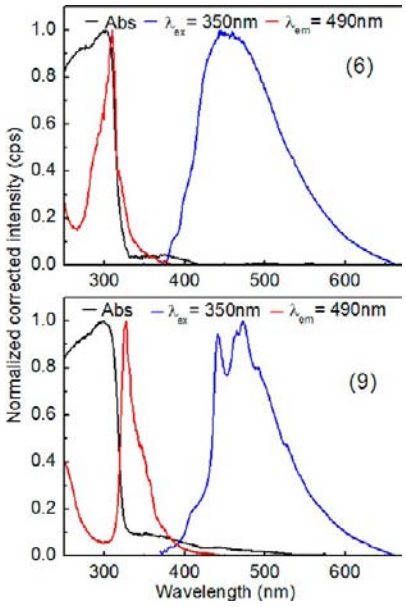

Figure 16. Solid state absorption (black), excitation (red), and emission (blue) of polymers **6** and **9** at 77 K. The sharper peaks are instrumental artifacts. These are emission peaks from the Xe lamp. Spectra measured on a different spectrometer do not show these features (see Experimental Section).

chain in the latter (Cu-S-S-Cu vs Cu-S-$(CH_2)_m$-S-Cu; m = 3, 5).[30] The most drastic difference between the photophysical behavior of this $[Cu_2I_2\{S(CH_2)_4S\}]_n$ polymer and those reported in this work ($[Cu_2I_2\{\mu$-ArS$(CH_2)_m$SAr$\}_2]_n$; Ar = Ph or tolyl; m = 3 or 5) is the presence of a low- and high-energy emission. Their presence resembles the photophysical behavior of the Cu_4I_4-containing materials, and one may suspect that a combination of rigidity and large T_1-T_2 energy gap, hence violating Kasha's rule, may explain the presence of two emissions. The current data bank on such rhombic Cu_2I_2-containing species is currently not large enough to firmly attest this hypothesis.

As for polymer **8**, despite the presence of only Cu_2I_2 units in the 2D polymer structure reported above, which should be characterized by an emission centered at 450 nm and a shorter lifetime (see data for polymers **1** and **5**), the emission lifetimes measured at 298 and 77 K are long reminiscent of the presence of the cubane Cu_4I_4-motif. On the basis of the spectra presented in Figure 14 and these long lifetimes we conclude that this polymer contains a mixture of polymers similar to polymers **4** and **5**. The shorter-lived component was not detected in the decays, probably because of the rather strong spectral overlap.

The Cu_2Br_2-containing polymers **3**, **6**, and **9** exhibit emission lifetimes well below the 1 μs time scale (i.e., ns and sub-ns), suggesting a particularly large rate for nonradiative processes. The decay traces for these polymers were found to be best described with two or three exponentials. The most important component is found to be very short (i.e., ps time-scale). This time scale is extraordinarily short for phosphorescence and one may suspect the presence of fluorescence. The spectral overlap between the lowest absorption and emission bands in the vicinity of 400 nm (Figure 16) is in line with this hypothesis. A strong fluorescence arising from binuclear copper complexes have been reported before ($[Cu_2(PhNNNPh)_2]$; $\tau_F \sim 1$ ns).[31] The presence of longer components (1.1−1.6 ns for **3**, **6**, and **9**, and 6.8 ± 0.5 ns for polymers **6** and **9**) suggests the presence of (weaker) phosphorescence as well, an emission that is not well

Table 1. Crystal Data, Data Collection, and Structure Refinement for 1, 2, 3, and 4

	1	2	3	4
formula	$C_{15}H_{16}CuIS_2$	$C_{30}H_{32}Cu_4I_4S_4$	$C_{75}H_{80}Cu_4Br_4S_{10}$	$C_{51}H_{60}Cu_4I_4S_6$
formula weight	450.84	1282.56	1875.79	1627.21
temperature/K	193	293	180	193
wavelength/Å	0.71073	0.71073	0.71073	0.71073
crystal system	orthorhombic	monoclinic	monoclinic	monoclinic
space group	*Pbca*	$P2_1/c$	$P2_1$	$C2/c$
a/Å	13.261(3)	12.595(2)	13.278(3)	29.557(6)
b/Å	14.189(3)	13.694(5)	21.664(2)	11.658(2)
c/Å	17.679(4)	22.386(4)	14.129(3)	19.257(4)
β/deg	90.00(1)	94.63(2)	107.72(1)	119.673(3)
volume/Å^3	3329.9 (12)	3848.4 (17)	3871.4(13)	5766.2(9)
Z	8	4	2	4
density (calculated) g/cm^3	1.799	2.214	1.609	1.875
absorption coefficient/mm^{-1}	3.401	5.626	3.459	3.847
F(000)	1760	2416	1892	3160
crystal size/mm	0.2, 0.2, 0.12	0.3, 0.25, 0.17	0.37, 0.32, 0.12	0.30, 0.20, 0.10
θ range for data collection/deg	2.30 to 25.00	3.54 to 30.06	3.03 to 32.07	2.05 to 25.00
index ranges	$-15 \le h \le 15$, $-16 \le k \le 16$, $-21 \le l \le 21$	$-17 \le h \le 17$, $-19 \le k \le 19$, $-25 \le l \le 31$	$-19 \le h \le 17$, $-32 \le k \le 31$, $-21 \le l \le 21$	$-35 \le h \le 35$, $-13 \le k \le 13$, $-22 \le l \le 22$
reflections collected	21437	68170	88180	17857
independent reflections	2928 [R(int) = 0.0858]	11156 [R(int) = 0.0792]	24862 [R(int) = 0.0553]	5070 [R(int) = 0.0857]
refinement method	full-matrix least-squares on F^2	full-matrix least-squares on F^2	full-matrix least-squares on F^2	full-matrix least-squares on F^2
data/restraints/parameters	2928/0/172	11156/0/379	24862/1/759	5070/0/245
goodness-of-fit on F^2	1.036	1.148	1.059	1.012
final R indices [$I > 2\sigma(I)$]	$R1$ = 0.0561, w$R2$ = 0.1238	$R1$ = 0.0423, w$R2$ = 0.0852	$R1$ = 0.0540, w$R2$ = 0.0865	$R1$ = 0.0742, w$R2$ = 0.1985
R indices (all data)	$R1$ = 0.0825, w$R2$ = 0.1316	$R1$ = 0.0718, w$R2$ = 0.1016	$R1$ = 0.1720, w$R2$ = 0.1242	$R1$ = 0.1024, w$R2$ = 0.2187
larg. diff. peak and hole/e Å^{-3}	1.174 and −1.007	0.877 and −1.124	2.713 and −1.105	3.100 and −1.312

dx.doi.org/10.1021/ic301385u | *Inorg. Chem.* 2012, 51, 9917−9934

Table 2. Crystal Data, Data Collection, and Structure Refinement for 5, 6, 8, and 9

	5	6	8	9
formula	$C_{17}H_{20}CuIS_2$	$C_{17}H_{20}BrCuS_2$	$C_{19}H_{24}CuIS_2$	$C_{19}H_{24}BrCuS_2$
formula weight	478.92	431.90	506.94	459.95
temperature/K	173	100	293	293
wavelength/Å	0.71073	0.71073	0.71073	0.71073
crystal system	monoclinic	monoclinic	monoclinic	triclinic
space group	$C2/c$	$C2/c$	$P2_1/c$	$P\bar{1}$
a/Å	17.755(7)	17.5702(13)	10.8493(9)	9.467(1)
b/Å	13.950(6)	13.6802(10)	9.2519(7)	9.609(1)
c/Å	15.212(7)	14.8649(11)	20.288(2)	12.326(2)
α/deg	90	90	90	76.22(2)
β/deg	109.898(10)	108.909(2)	97.23(1)	67.90(2)
γ/deg	90	90	90	85.26(2)
volume/ Å^3	3543(3)	3380.2(4)	2020.2(3)	1009.0(2)
Z	8	8	4	2
density (calculated) g/cm^3	1.796	1.697	1.667	1.514
absorption coefficient/mm^{-1}	3.202	3.894	2.813	3.266
F(000)	1888	1744	1008	468
Crystal size/mm	0.3, 0.3, 0.2	0.36, 0.38, 0.47	0.54, 0.54, 0.46	0.46, 0.33, 0.19
Theta range for data collection/°	2.11 to 27.00	2.08 to 35.00	1.89 to 26.05	1.83 to 25.95
index ranges	$-17 \le h \le 22$, $-17 \le k \le 17$, $-11 \le l \le 19$	$-28 \le h \le 28$, $-22 \le k \le 22$, $-24 \le l \le 24$	$-13 \le h \le 13$, $-11 \le k \le 11$, $-24 \le l \le 24$	$-11 \le h \le 11$, $-11 \le k \le 11$, $-14 \le l \le 15$
reflections collected	9809	52337	19134	11689
independent reflections	3725 [R(int) = 0.0257]	7811 [R(int) = 0.0590]	3953 [R(int) = 0.0808]	3641 [R(int) = 0.0567]
refinement method	full-matrix least-squares on F^2	full-matrix least-squares on F^2	full-matrix least-squares on F^2	full-matrix least-squares on F^2
data/restraints/parameters	3725/0/191	7811/0/192	3953/0/211	3641/0/210
goodness-of-fit on F^2	1.039	1.033	1.045	0.850
final R indices [$I > 2\sigma(I)$]	$R1$ = 0.0271, w$R2$ = 0.0667	$R1$ = 0.0184, w$R2$ = 0.0514	$R1$ = 0.0415, w$R2$ = 0.1089	$R1$ = 0.0307, w$R2$ = 0.0601
R indices (all data)	$R1$ = 0.0361 w$R2$ = 0.0700	$R1$ = 0.0218 w$R2$ = 0.5223	$R1$ = 0.0498, w$R2$ = 0.1138	$R1$ =0.0630, w$R2$ = 0.0658
larg. diff. peak and hole/e Å^{-3}	0.701 and −0.411	0.617 and −0.849	1.045 and −0.884	0.443 and −0.357

Table 3. Emission Lifetimes Acquired for the Solid Polymers at Both 77 and 298 K

	298 K		77 K	
polymer	λ_{em} (nm)	τ_e (μs)	λ_{em} (nm)	τ_e (μs)
1	440	0.59 ± 0.01	440	0.67 ± 0.01
2	*a*	*a*	420	0.60 ± 0.01
	520	1.64 ± 0.01	525	6.03 ± 0.10
4	*a*	*a*	420	0.59 ± 0.01
	560	1.04 ± 0.05	555	8.04 ± 0.01
5	440	0.60 ± 0.05	440	1.39 ± 0.10
8[b]	545	1.22 ± 0.02	535	8.74 ± 0.03
3	480	0.00015 (97%)	490	0.00020 (99%)
		0.0011 (3%)		0.0016 (1%)
6	*a*	*a*	470	0.00002 (81%)[c]
				0.0011 (15%)
				0.0063 (4%)
9	*a*	*a*	470	0.00024 (62%)[c]
				0.0011 (29%)
				0.0073 (9%)

[a]Not observed. [b]Due to Cu_4I_4-containing polymer as a minor contamination product. [c]No uncertainty was evaluated.

separated in the spectra, but rather is overlapping strongly with the suspected fluorescence. A closely spaced dual emission, fluorescence and phosphorescence, was also detected for an Au(I)···Au(I) species built upon a Cl−Au−S═C(SR)$_2$ motif was also recently reported (T = 77 K in 2-methyltetrahydrofuran: λ_{fluo} = 510 nm (shoulder); τ_F = 1.38 ± 0.02 ns; λ_{phos} = 580 nm; τ_P = 676 ± 13 μs)[32] Noteworthy in this case, the particularly long fluorescence lifetime (1.4 ns) is in line with the long phosphorescence lifetime as well. Other examples of gold(I) fluorescing species exist,[33] and one cannot neglect this possibility. Time-resolved spectroscopy was used in an attempt to detect longer lived species, notably in the μs time scale, but none were observed. Similarly, this technique was also employed to distinguish between the two ns components, but failed because of the weakness of the noisy signal.

For these Cu_2Br_2-containing polymers, the weak emission intensities corroborate the very short lifetimes for the luminescence, and again, strongly suggest the presence of very efficient non-radiative processes. Because we also find no reports on the emission of Cu_2Cl_2-containing materials, one can only suspect that the Cu-X bond (presumably the relative Cu-X bond strength) plays a major role in defining the photophysical properties of these materials.

The series would be completed if the corresponding cubane-type Cu_4Br_4 would be obtained as well. This was not the case. The closest system concerns the open cubane structure for the (Cu_4Br_4) unit reported for a polymer described as $[(Cu_4Br_4)(Cu_2Br_2)(SEt_2)_3]_n$. In this case, two emissions were depicted at 425 (τ_e = 0.89 ± 0.01 μs, 298 K) and 440 nm (τ_e = 2.53 ± 0.05 μs, 77 K), and at 550 nm (τ_e = 0.78 ± 0.01 μs, 298 K; τ_e = 1.47 ± 0.02 μs, 77 K).[22] The long emission lifetimes are most certainly consistent with the particularly rigid MOF of this material. On the basis of the current findings on the Cu_2Br_2-containing polymers, the observed dual emission in this mixed cluster polymer that was first thought to be associated with the individual (Cu_4Br_4) and (Cu_2Br_2) components may be due to the former unit only,

dx.doi.org/10.1021/ic301385u | Inorg. Chem. 2012, 51, 9917−9934

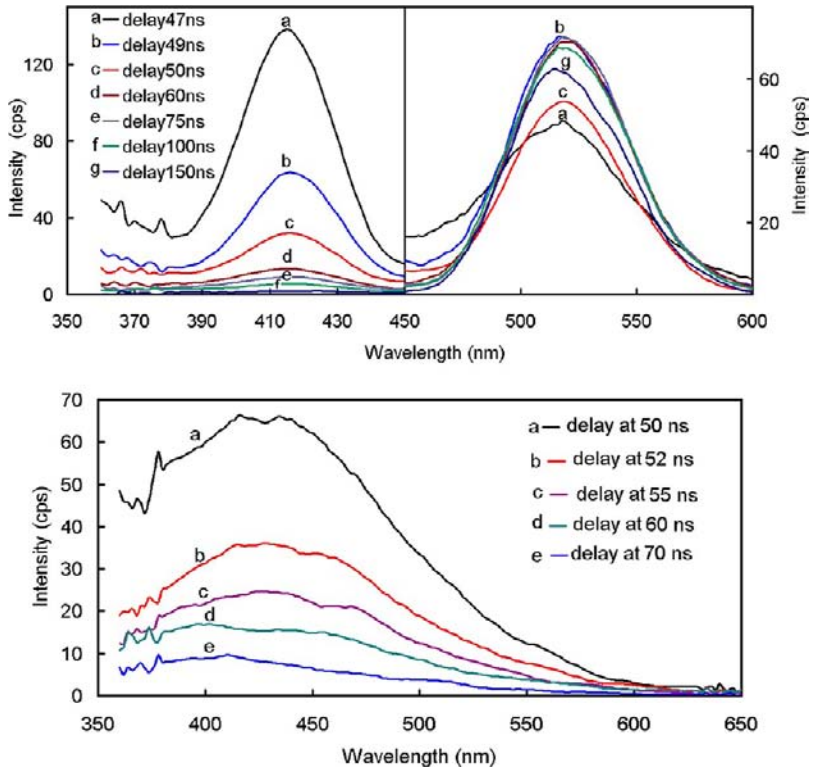

Figure 17. Top: time-resolved spectra of solid $[Cu_4I_4\{\mu\text{-PhS}(CH_2)_3SPh\}_2]_n$ (**2**) at 77 K with λ_{exc} = 350 nm at different delay times. Bottom: time-resolved spectra of solid $[(CuI)_2\{\mu\text{-PhS}(CH_2)_5SPh\}_2]_n$ (**5**) at 77 K with excitation at 350 nm at different delay times.

because the relatively long emission lifetimes (μs time scale) for both emissions compare far better to those obtained for the cubane-type materials (Cu_4I_4) than those obtained for the rhombic (Cu_2Br_2) ones. To verify this suspicion, polymers solely built upon (Cu_4Br_4) units need to be prepared and investigated.

CONCLUSION

This study shows that the outcome of the self-assembly process between CuI and $ArS(CH_2)_mSAr$ ligands is hardly predictable. Whereas the nuclearity and dimensionality of the resulting MOFs are neither affected by the metal-to-ligand ratio nor the nature of Ar (Ph vs *p*-Tol) in the case of $ArSCH_2SAr$,[13] this work has established that in the case of $ArS(CH_2)_3SAr$ and $ArS(CH_2)_5SAr$ the variation of these parameter may have a crucial role on composition and topology of the polymeric materials. Even a small change of the steric demand of the aryl groups (Ph vs *p*-Tol), which appear as "innocent" at the first glance, alters significantly the structural features of the networks. However, our comparative work confirms that treatment of CuI with $ArS(CH_2)_mSAr$ (m = 1, 3, 4, 5) in a 2:1 metal-to-ligand ratio generally gives rise to networks incorporating Cu_4I_4 clusters as SBUs, whereas formation of MOFs with $Cu(\mu_2\text{-I})_2Cu$ units is most often observed upon reacting these dithioether with CuI in a 1:1 ratio. Nontheless, some exceptions from this tendency, for example, with the *p*-$TolS(CH_2)_4STol$-*p* ligand, have been encountered.[13b] This study has furthermore demonstrated, that the nature of the halide ligand plays also an important role. This structural variety has an impact on the mean Cu···Cu distances, which lie in the range between 2.75−3.05 Å, thus influencing also the luminescence properties. The solid-state luminescence spectra at 298 and 77 K of **2** and **4** exhibit very strong emissions around 535 and 560 nm, respectively, with emission lifetime >1.0 μs typical for Cu_4I_4-type materials. The Cu_2I_2-type polymers, **1** and **5**, display weaker signals at ∼450 nm with emission lifetimes 0.6−1.4 μs. The number of examples of such motif to be reported for their photophysical properties is still scarce. Polymer **8** is found to be contaminated by cubane-containing materials, presumably polymer **7**. The Br-containing species are also found to be weakly luminescent centering around 450−475 nm. Such examples are rare, and the report for luminescence properties for these species is unprecedented. Their lifetime decays exhibit multiple components, some of which are particularly short-lived (ps time scale) strongly suggesting the presence of fluorescence, combined with a strongly overlapping phosphorescence (ns time scale). We have now started the systematic construction of a data bank for structures and photophysical properties of $(Cu_2X_2)_n$-type materials (X = Br, I; n = 1, 2 (and 3 see reference 13a)). A systematic variation of the $(CH_2)_m$ chain length and relative rigidity is now the next logical step toward the full understanding of these luminescent materials. One of the key parameters that is becoming now more obvious is the polymer rigidity effect on the properties.

EXPERIMENTAL SECTION

Materials. CuI, CuBr and 1,3-bis(phenylthio)propane was purchased from Acros, and 1,5-bis(phenylthio)pentane and 1,5-bis(*p*-tolylthio)pentane were prepared as described in the literature.[34]

Preparation of Polymer 1. To a solution of CuI (191 mg, 1.0 mmol) in MeCN (10 mL) was added $PhS(CH_2)_3SPh$ (286 mg/253 μL, 1.1 mmol). After stirring for 1 h, the mixture refluxed for 5 min until all material redissolved. Upon cooling, large colorless blocks of **1** were formed and separated after 2 d. Yield (78%). Anal. Calcd. for $C_{30}H_{32}Cu_2I_2S_4$ (901.75): C, 39.96; H, 3.58; S, 14.22. Found: C, 39.62; H, 3.36; S, 13.95.

Preparation of Polymer 2. To a solution of CuI (802 mg, 2.1 mmol) in MeCN (20 mL) was added $PhS(CH_2)_3SPh$ (261 mg/231 μL, 1 mmol) dissolved in 5 mL of MeCN. Slow addition of the ligand and the use of a slight excess of CuI are necessary to minimize competing

dx.doi.org/10.1021/ic301385u | Inorg. Chem. 2012, 51, 9917−9934

formation of compound **1**. The mixture was first stirred overnight at room temperature. Partial precipitation of the white polymer occurred after several hours. The mixture was refluxed for 2 min until all material redissolved, the solution was then allowed to reach slowly room temperature. After one day, colorless crystals of **1** formed and were filtered off. A second crop could be isolated after keeping the filtered solution in refrigerator a 7 °C. The crystalline sample contained some crystals of weakly luminescent compound **1**, which were separated manually under a UV lamp at 366 nm. Overall yield (52%). No satisfactory elemental analysis could be obtained, most probably because of contamination with small amounts of **1**, but the obtained values are nevertheless close to a CuI-to-ligand ration of 2:1.

Preparation of Polymer 3. In a Schlenk tube CuBr (143 mg, 1.0 mmol) was dissolved under Ar atmosphere in degassed MeCN (8 mL) and $PhS(CH_2)_3SPh$ (286 mg/253 μL, 1.1 mmol) was added. After stirring for 1 h, the greenish solution was stored for 1 d in a refrigerator a 5 °C. Large brownish blocks of **3** were formed progressively and separated after 2 d. Yield (43%). Anal. Calcd. for $C_{30}H_{32}Br_4Cu_2S_4$ x 0.5 $C_{15}H_{16}S_2$ (937.96): C, 48.02; H, 4.30; S, 17.10. Found: C, 27.82; H, 4.36; S, 16.90

Preparation of Polymer 4. To a solution of CuI (802 mg, 2.1 mmol) in MeCN (20 mL) was added $PhS(CH_2)_5SPh$ (285 mg, 1 mmol) dissolved in 5 mL of MeCN. Slow addition of the ligand and the use of a slight excess of CuI are necessary to minimize competing formation of compound **5**. The mixture was first stirred overnight at room temperature. Partial precipitation of the white polymer occurred after several hours. The mixture was refluxed for 2 min until all material redissolved, the solution was then allowed to reach room temperature slowly. After one day, colorless crystals of **4** formed and were filtered off. A second crop could be isolated after keeping the filtered solution in refrigerator a 5 °C. The crystalline sample contained some crystals of weakly luminescent compound **5**, which were separated manually under a UV lamp at 366 nm. Overall yield (41%). No satisfactory elemental analysis could be obtained, most probably because of contamination with small amounts of **5**.

Preparation of Polymer 5. To a solution of CuI (191 mg, 1.0 mmol) in MeCN (10 mL) was added $PhS(CH_2)_5SPh$ (317 mg, 1.1 mmol). After stirring for 1 h, the mixture was refluxed for 5 min until all material redissolved. Upon cooling large colorless blocks of **5** were formed and separated after 2 d. Yield (73%). Anal. Calcd. for $C_{34}H_{40}Cu_2I_2S_4$ (957.86): C, 42.63; H, 4.21; S, 13.39. Found: C, 42.32; H, 3.98; S, 13.02.

Preparation of Polymer 6. $PhS(CH_2)_5SPh$ (317 mg, 1.1 mmol) was dissolved in degassed MeCN (10 mL) under Ar atmosphere in a Schlenk tube, and CuBr (143 mg, 1.0 mmol) was added. After stirring for 1 h, the greenish solution was stored for 1 d in a refrigerator at 5 °C. Large colorless blocks of **6** were formed progressively and separated after 2 d. Yield (77%). Anal. Calcd. for $C_{34}H_{40}Br_2Cu_2S_4$ (863.86): C, 47.27; H, 4.67; S, 14.85. Found: C, 47.02; H, 4.98; S, 13.02.

Preparation of Polymer 8. To a solution of CuI (191 mg, 1.0 mmol) in MeCN (10 mL) was added *p*-$TolS(CH_2)_5STol$-*p* (348 mg, 1.1 mmol). After stirring for 1 h, the mixture was refluxed for 5 min until all material redissolved. Upon cooling colorless crystals of **8** were formed and separated after 2 d. Yield (81%). Anal. Calcd for $C_{38}H_{48}Cu_2I_2S_4$ (1013.96): C, 45.01; H, 4.77; S, 12.65. Found: C, 44.72; H, 4.43; S, 12.32.

Preparation of Polymer 9. This compound was prepared as described for **6**. Yield (71%). Anal. Calcd for $C_{38}H_{48}Br_2Cu_2S_4$ (919.96): C, 49.61; H, 5.26; S, 13.94. Found: C, 49.82; H, 5.43; S, 13.62.

Instruments. The UV−vis spectra were recorded on a Varian Cary 50 spectrophotometer. Emission and excitation spectra were obtained by using a double monochromator Fluorolog 2 instrument from Spex. Fluorescence lifetimes were measured on a Timemaster model TM-3/2003 apparatus from PTI. The source was a nitrogen laser equipped with a high-resolution dye laser (fwhm ~1400 ps), and the fluorescence lifetimes were obtained from deconvolution and distribution lifetime analysis. For polymers **6** and **9**, the very short lifetimes were acquired using a QM-40 steady-state fluorometer from PTI using the PicoMaster 1 TCSPC upgrade. The light source: was a pulsed 375 nm picosecond laser diode (fwhm = 250 ps) and the detector was a PMD-2 fast pmt. The TGA traces were acquired on a Perkin-Elmer TGA 7 apparatus in the temperature range between 50 and 950 °C at 3°/ min under a nitrogen atmosphere. The spectra of polymers 6 and 9 were also measured on a QM-40 steady-state fluorometer using a 75 W xenon lamp and a 914 multimode detector with R928 pmt in photon counting mode was used.

X-ray Crystallography. Information concerning the data collection and processing, crystallographic parameters, and details on structure solution and refinement are given in Table 1. X-ray single-crystal diffraction data were collected at 293 K for **2** and 180 K for **3** on a BRUKER KappaCCD diffractometer, equipped with a graphite monochromator utilizing Mo$K\alpha$ radiation (λ = 0.71073 Å). The structures were solved by direct methods and expanded using Fourier techniques for **3**. Refinements were performed on F^2 by full matrix least-squares techniques using SHELXL-97 program (G.M. Sheldrick, 1998). All non-hydrogen atoms were refined anisotropically except for C atoms of the isolated ligand for **3**, which were refined isotropically. Absorption was corrected by SADABS program (Sheldrick, Bruker, 2008), and the H atoms were included in the calculation without refinement. For **3**, a statistical disorder on the propane part of the isolated ligand was applied to lead to occupation rate of 0.5 for C73, C74, C76, and C77. Also one of the rings of this isolated ligand (C61−C66) was regularized to idealized planar ring to avoid the distortion of the ring. The data for **1**, **5**, **8**, and **9** (Table 2) were collected at 173 and 293 K on a STOE IPDS diffractometer equipped with a graphite monochromator utilizing Mo$K\alpha$ radiation (λ = 0.71073 Å). The structures were solved by direct methods using SIR92[35] and refined on F^2 by full-matrix least-squares method, using SHELXL-97 (G. M. Sheldrick, 1998). Non-hydrogen atoms were refined anisotropically and absorption was corrected by Gaussian technique for **8** and **9**. The H atoms were included in the calculation without refinement. A numerical absorption correction using the FACEIT program in IPDS (Stoe & Cie, 1999) was employed for **1** and **5**. X-ray single-crystal diffraction data for **4** were collected at 193 K on a Bruker APEX diffractometer (D8 three-circle goniometer, type of radiation: Mo−Kα, λ = 0.71073 Å). (Bruker AXS); data collection, cell determination and refinement: Smart version 5.622 (Bruker AXS, 2001); integration: SaintPlus version 6.02 (Bruker AXS, 1999); empirical absorption correction: SADABS version 2.01 (Bruker AXS, 1999). The structure was solved applying direct and Fourier methods, using SHELXS-90 and SHELXL-97 (G. M. Sheldrick, SHELXL-97).[36] The X-ray intensity data of **6** were measured at 100 K on a Bruker Kappa APEX II CCD system equipped with a TRIUMPH curved-crystal monochromator and a Mo fine-focus tube (λ = 0.71073 Å). A total of 3423 frames were collected. The frames were integrated with the Bruker SAINT software package using a narrow-frame algorithm The structure of **6** was solved and refined using the Bruker SHELXTL Software Package. Data were corrected for absorption effects using the multiscan method (SADABS).

■ ASSOCIATED CONTENT

Ⓢ Supporting Information

X-ray crystallographic data in CIF format, view of the dinuclear Cu_2I_2 core of **1** with the numbering scheme, packing diagram of **4** and a perspective view down the *c* axis of **2**, graphs of the 1st derivative of the TGA traces, and photographs showing the solid-state luminescence of **7**. This material is available free of charge via the Internet at http://pubs.acs.org.

■ AUTHOR INFORMATION

Corresponding Author

*E-mail: michael.knorr@univ-fcomte.fr (M.K.), pierre.harvey@usherbrooke.ca (P.D.H.).

Notes

The authors declare no competing financial interest.

⊥On leave from the Chemistry Department, Assiut University, Assiut, Egypt.

■ ACKNOWLEDGMENTS

This research was supported by the CNRS and the Natural Sciences and Engineering Research Council of Canada (NSERC), le Fonds Québécois de la Recherche sur la Nature et les Technologies (FQRNT), the Centre Québécois des Matériaux Fonctionnels (CQMF), and the Centre d'Études des Matériaux Optiques et Photoniques de l'Université de Sherbrooke (CEMOPUS). P.D.H. thanks Dr. Alex Siemarziuk from Photon Technology Inc (London, Ontario) for the kind measurements of the emission spectra and lifetimes for polymers **6** and **9** at 77 K.

■ DEDICATION

This article is dedicated to Professor Dieter Fenske on the occasion of his 70th birthday.

■ REFERENCES

(1) (a) Valderrama, M.; Contreras, R.; Arancibia, V.; Boys, D. *J. Organomet. Chem.* **2001**, *620*, 256−262. (b) Chiffey, A. F.; Evans, J.; Levason, W.; Webster, M. *J. Chem. Soc., Dalton Trans.* **1994**, 2835−2840. (c) Awaleh, M. O.; Badia, A.; Brisse, F. *Acta Crystallogr.* **2005**, *E61*, m1586−m1587.

(2) Bu, X.-H.; Chen, W.; Du, M.; Biradha, K.; Wang, W.-Z.; Zhang, R.-H. *Inorg. Chem.* **2002**, *41*, 437−439.

(3) (a) Black, J. R.; Levason, W. *J. Chem. Soc., Dalton Trans.* **1994**, 3225−3230. (b) Dann, S. E.; Genge, A. R. J.; Levason, W.; Reid, G. *J. Chem. Soc., Dalton Trans.* **1996**, 4471−4478. (c) Li, J.-R.; Du, M.; Zhang, R.-H.; Bu, X.-H. *J. Mol. Struct.* **2002**, *607*, 175−179. (d) Collin, J.-P.; Jouvenot, D.; Koizumi, M.; Sauvage, J.-P. *Inorg. Chim. Acta* **2007**, *360*, 923−930.

(4) Awaleh, M. O.; Baril-Robert, F.; Reber, C.; Badia, A.; Brisse, F. *Inorg. Chem.* **2008**, *47*, 2964−2974.

(5) Sanger, A. R.; Weiner-Fedorak, J. E. *Inorg. Chim. Acta* **1980**, *42*, 101−103.

(6) Xie, Y.-B.; Li, J.-R.; Zheng, Y.; Bu, X.-H.; Zhang, R.-H. *J. Mol. Struct.* **2003**, *645*, 227−230.

(7) (a) Chen, W.; Du, M.; Zhang, R. H.; Bu, X. H. *Acta Crystallogr.* **2001**, *E57*, m213−m215. (b) Bu, X.-H.; Hou, W.-F.; Du, M.; Chen, W.; Zhang, R.-H. *Cryst. Growth Des.* **2002**, *2*, 303−307.

(8) Li, J.-R.; Bu, X.-H. *Eur. J. Inorg. Chem.* **2008**, 27−40.

(9) (a) Schramm, V.; Fischer, K. F. *Naturwissenschaften* **1974**, *61*, 500−501. (b) Raston, C. L.; White, A. H. *J. Chem. Soc., Dalton Trans.* **1976**, 2153−2156. (c) Hardt, H. D.; Pierre, A. *Inorg. Chim. Acta* **1977**, *25*, L59−L60. (d) Eitel, E.; Oelkrug, D.; Hiller, W.; Straehle, J. *Z. Naturforsch.* **1980**, *35B*, 1247−53. (e) Rath, N. P.; Holt, E. M.; Katsumi, T. *Inorg. Chem.* **1985**, *24*, 3934−3938. (f) Hu, G.; Mains, G. J.; Holt, E. M. *Inorg. Chim. Acta* **1995**, *240*, 559−565. (g) Cariati, E.; Bourassa, J.; Ford, P. C. *Chem. Commun.* **1998**, 1623−1624. (h) Hu, S.; Tong, M.-L. *Dalton Trans.* **2005**, 1165−1167. (i) Li, T.; Du, S.-W. *J. Cluster. Sci.* **2008**, *19*, 323−330. (j) Ren, S.-B.; Zhou, L.; Zhang, J.; Li, Y.-Z.; Du, H.-B.; You, X.-Z. *CrystEngComm* **2009**, *11*, 1834−1836. (k) Braga, D.; Maini, L.; Mazzeo, P. P.; Ventura, B. *Chem.—Eur. J.* **2010**, *16*, 1553−1559. (l) Manbeck, G. F.; Brennessel, W. W.; Evans, C. M.; Eisenberg, R. *Inorg. Chem.* **2010**, *49*, 2834−2843. (m) Zhang, Y.; He, X.; Zhang, J.; Feng, P. *Cryst. Growth Des.* **2011**, *11*, 29−32. (n) Jalilian, E.; Liao, R.-Z.; Himo, F.; Lidin, S. *Mater. Res. Bull.* **2011**, *46*, 1192−1196. (o) Parmeggiani, F.; Sacchetti, A. *J. Chem. Educ.* **2012**, *89*, 946−949. (p) Gschwind, F.; Sereda, O.; Fromm, K. M. *Inorg. Chem.* **2009**, *48*, 10535−10547.

(10) (a) Dyason, J. C.; Healy, P. C.; Engelhardt, L. M.; Pakawatchai, C.; Patrick, V. A.; Raston, C. L.; White, A. H. *J. Chem. Soc., Dalton Trans.* **1985**, 831−838. (b) Engelhardt, L. M.; Healy, P. C.; Kildea, J. D.; White, A. H. *Aust. J. Chem.* **1989**, *42*, 107−113. (c) Altaf, M.; Stoeckli-Evans, H. *Inorg. Chim. Acta* **2010**, *363*, 2567−2573. (d) Kitagawa, H.; Ozawa, Y.; Toriumi, K. *Chem.Commun.* **2010**, *46*, 6302−6304. (e) Perruchas, S.; Tard, C. d.; Le Goff, X. F.; Fargues, A.; Garcia, A.; Kahlal, S.; Saillard, J.-Y.; Gacoin, T.; Boilot, J.-P. *Inorg. Chem.* **2011**, *50*, 10682−10692. (f) Roppolo, I.; Celasco, E.; Fargues, A.; Garcia, A.; Revaux, A.; Dantelle, G.; Maroun, F.; Gacoin, T.; Boilot, J.-P.; Sangermano, M.; Perruchas, S. *J. Mater. Chem.* **2011**, *21*, 19106−19113. (g) Liu, Z.; Djurovich, P. I.; Whited, M. T.; Thompson, M. E. *Inorg. Chem.* **2011**, *51*, 230−236.

(11) (a) Rath, N. P.; Holt, E. M.; Tanimura, K. *J. Chem. Soc., Dalton Trans.* **1986**, 2303−2310. (b) Caradoc-Davies, P. L.; Hanton, L. R.; Hodgkiss, J. M.; Spicer, M. D. *J. Chem. Soc., Dalton Trans.* **2002**, 1581−1585. (c) Muthu, S.; Ni, Z.; Vittal, J. J. *Inorg. Chim. Acta* **2005**, *358*, 595−605. (d) Shi, W.-J.; Ruan, C.-X.; Li, Z.; Li, M.; Li, D. *CrystEngComm* **2008**, *10*, 778−783. (e) Deng, Z.-P.; Qi, H.-L.; Huo, L.-H.; Ng, S. W.; Zhao, H.; Gao, S. *Dalton Trans.* **2010**, *39*, 10038−10050.

(12) (a) Peindy, H. N.; Guyon, F.; Khatyr, A.; Knorr, M.; Strohmann, C. *Eur. J. Inorg. Chem.* **2007**, 1823−1828. (b) Knorr, M.; Guyon, F.; Khatyr, A.; Däschlein, C.; Strohmann, C.; Aly, S. M.; Abd-El-Aziz, A. S.; Fortin, D.; Harvey, P. D. *Dalton Trans.* **2009**, 948−955.

(13) (a) Harvey, P. D.; Knorr, M. *Macromol. Rapid Commun.* **2010**, *31*, 808−826. (b) Knorr, M.; Guyon, F. Luminescent Oligomeric and Polymeric Copper Coordination Compounds Assembled by Thioether Ligands. In *Macromolecules Containing Metal and Metal-like Elements*; Abd-El Aziz, A. S., Carraher, C. E., Pittmann, C. U., Zeldin, M., Eds.; John Wiley & Sons, Inc: New York, 2010; Photophysics and Photochemistry of Metal-containing Polymers, Vol. *10*, Chapter 3, pp 89−158.

(14) (a) Kim, T. H.; Lee, K. Y.; Shin, Y. W.; Moon, S.-T.; Park, K.-M.; Kim, J. S.; Kang, Y.; Leea, S. S.; Kim, J. *Inorg. Chem. Commun.* **2005**, *8*, 27−30. (b) Kim, T. H.; Shin, Y. W.; Lee, S. S.; Kim, J. *Inorg. Chem. Commun.* **2007**, *10*, 11−4. (c) Kim, T. H.; Park, G.; Shin, Y. W.; Park, K.-M.; Choi, M. Y.; Kim, J. *Bull. Korean Chem. Soc.* **2008**, *29*, 499−502. (d) Xie, C.; Zhou, L.; Feng, W.; Wang, J.; Chen, W. *J. Mol. Struct.* **2009**, *921*, 132−136. (e) Zhang, J.; Xue, Y.-S.; Li, Y.-Z.; Du, H.-B.; You, X.-Z. *CrystEngComm* **2011**, *13*, 2578−2585. (f) Kim, T. H.; Yang, H.; Park, G.; Lee, K. Y.; Kim, J. *Chem.—Asian J.* **2010**, *5*, 252−255.

(15) For examples of Cu_nX_n compounds ligated by macrocyclic thioether ligands see: (a) Ashton, P. R.; Burns, A. L.; Claessens, C. G.; Shimizu, G. K. H.; Small, K.; Stoddard, J. F.; White, A. J. P.; Williams, D. J. *J. Chem. Soc., Dalton Trans.* **1997**, 1493−1496. (b) Lucas, C. R.; Liang, W.; Miller, D. O.; Bridson, J. N. *Inorg. Chem.* **1997**, *36*, 4508−4513. (c) Kim, H. J.; Song, M. R.; Lee, S. Y.; Young, J.; Shim, L.; Lee, S. *Eur. J. Inorg. Chem.* **2008**, 3532−3539. (d) Lee, J. Y.; Lee, S. Y.; Sim, W.; Park, K.-M.; Kim, J.; Lee, S. S. *J. Am. Chem. Soc.* **2008**, *130*, 6902−6903. (e) Jin, Y.; Kim, H. J.; Lee, J. Y.; Lee, S. Y.; Shim, W. J.; Hong, S. H.; Lee, S. S. *Inorg. Chem.* **2010**, *49*, 10241−10243. (f) Park, I.-H.; Lee, S. S. *CrystEngComm* **2011**, *13*, 6520−6525. (g) Heller, M.; Sheldrick, W. S. *Z. Anorg. Allg. Chem.* **2003**, *629*, 1589−1595. (h) Heller, M. *Z. Anorg, Allg. Chem.* **2006**, *632*, 441−444. (i) Jo, M.; Seo, J.; Lindoy, L. F.; Lee, S. S. *Dalton Trans.* **2009**, 6096−6098.

(16) (a) Toyota, S.; Matsuda, Y.; Nagaoka, S.; Oki, M.; Akashi, H. *Bull. Chem. Soc. Jpn.* **1996**, *69*, 3115−3121. (b) The reaction of CuBr with $EtS(CH_2)_4SEt$ is reported to give an adduct $[Cu_2Br_2\{EtS(CH_2)_4SEt\}]$ (based on elemental analyses) of unknown structure: Ainscough, E. W.; Brodie, A. M.; Husbands, J. M.; Gainsford, G. J.; Gabe, E. J.; Curtis, N. F. *J. Chem. Soc., Dalton Trans.* **1985**, 151−158.

(17) Brooks, N. R.; Blake, A. J.; Champness, N. R.; Cooke, P. A.; Hubberstey, P.; Proserpio, D. M.; Wilson, C.; Schröder, M. *J. Chem. Soc., Dalton Trans.* **2001**, 456−465.

(18) Yim, H. W.; Rabinovich, D.; Lam, K. C.; Golen, J. A.; Rheingold, A. L. *Acta Crystallogr.* **2003**, *E59*, m556−m558.

(19) Lu, W.; Yan, Z.-M.; Dai, J.; Zhang, Y.; Zhu, Q.-Y.; Jia, D.-X.; Guo, W.-J. *Eur. J. Inorg. Chem.* **2005**, 2339−2345.

(20) Noren, B.; Oskarsson, A. *Acta Chem. Scand.* **1987**, *A41*, 12−17.

(21) For a CuBr-based 1D coordination polymer linked by a tridentate thioether ligand see: Yim, H. W.; Tran, L. M.; Pullen, E. E.; Rabinovich, D.; Liable-Sands, L. M.; Concolino, T. E.; Rheingold, A. L. *Inorg. Chem.* **1999**, *38*, 6234−6239.

(22) Knorr, M.; Pam, A.; Khatyr, A.; Strohmann, C.; Kubicki, M. M.; Rousselin, Y.; Aly, S. M.; Fortin, D.; Harvey, P. D. *Inorg. Chem.* **2010**, *49*, 5834−5844.

(23) San Filippo, J., Jr.; Zyontz, L. E.; Potenza, J. *Inorg. Chem.* **1975**, *14*, 1667−1671.

(24) Martinez-Alanis, P. R.; Ugalde-Saldivar, V. M.; Castillo, I. *Eur. J. Inorg. Chem.* **2011**, 212−220.
(25) Knorr, M.; Guyon, F.; Kubicki, M. M.; Rousselin, Y.; Aly, S. M.; Harvey, P. D. *New J. Chem.* **2011**, *35*, 1184−1188.
(26) Kim, T. H.; Shin, Y. W.; Jung, J. H.; Kim, J. S.; Kim, J. *Angew. Chem., Int. Ed.* **2008**, *47*, 685−688.
(27) Munakata, M.; Wu, L. P.; Kuroda-Sowa, T.; Maekawa, M.; Suenaga, Y.; Nakagawa, S. *J. Chem. Soc., Dalton Trans.* **1996**, 1525−1530.
(28) (a) Angelis, F. D.; Fantacci, S.; Sgamellotti, A.; Cariati, E.; Ugo, R.; Ford, P. C. *Inorg. Chem.* **2006**, *45*, 10576−10584. (b) Vitale, M.; Ryu, C. K.; Palke, W. E.; Ford, P. C. *Inorg. Chem.* **1994**, *33*, 561−566.
(29) For reviews on the photophysics of Cu(I) compounds see: (a) Ford, P. C.; Cariati, E.; Bourassa, J. *Chem. Rev.* **1999**, *99*, 3625−3648. (b) Armaroli, N.; Accorsi, G.; Cardinali, F.; Listorti, A. *Top. Curr. Chem.* **2007**, *280*, 69−115.
(30) Knorr, M.; Guyon, F.; Khatyr, A.; Allain, M.; Aly, S. M.; Lapprand, A.; Fortin, D.; Harvey, P. D. *J. Inorg. Organomet. Polym. Mater.* **2010**, *20*, 534−43.
(31) Harvey, P. D. *Inorg. Chem.* **1995**, *34*, 2019−2024.
(32) Guyon, F.; Hameau, A.; Khatyr, A.; Knorr, M.; Amrouche, H.; Fortin, D.; Harvey, P. D.; Strohmann, C.; Ndiaye, A. L.; Huch, V.; Veith, M.; Avarvari, N. *Inorg. Chem.* **2008**, *47*, 7483−492.
(33) Lee, Y.-A.; McGarrah, J. E.; Lachicotte, R. J.; Eisenberg, R. *J. Am. Chem. Soc.* **2002**, *124*, 10662−10663.
(34) (a) Siedlecka, R.; Skarzewski, J. *Synthesis* **1994**, 401−404. (b) Brito, I.; Cardenas, A.; Albanez, J.; Bolte, M.; Lopez-Rodriguez, M. *Acta Crystallogr.* **2009**, *E65*, o2980.
(35) Altomare, A.; Cascarano, G.; Giacovazzo, C.; Gualardi, A. *J. Appl. Crystallogr.* **1993**, *26*, 343−350.
(36) Sheldrick, G. M. *Acta Crystallogr.* **2008**, *A64*, 112−122.